Student thesis series INES 555

Traits of peat- and upland-derived stream dissolved organic carbon in the permafrost region around Abisko, northern Sweden

Nora Kainz

2021
Department of
Physical Geography and Ecosystem Science
Lund University
Sölvegatan 12
S-223 62 Lund
Sweden

Nora Kainz
Traits of peat- and upland-derived stream dissolved organic carbon in the permafrost region around Abisko, northern Sweden
Master degree thesis, 30 credits in *Atmospheric Sciences and Biogeochemical Cycles*
Department of Physical Geography and Ecosystem Science, Lund University

Level: Master of Science (MSc)

Course duration: *January* 2021 until *June* 2021

Disclaimer

Traits of peat- and upland-derived stream dissolved organic carbon in the permafrost region around Abisko, northern Sweden

---

Nora Kainz

Master thesis, 30 credits, in *Atmospheric Sciences and Biogeochemical Cycles*

Supervisor 1: Martin Berggren
Department of Physical Geography and Ecosystem Science,
University of Lund

Supervisor 2: Andreas Persson
Department of Physical Geography and Ecosystem Science,
University of Lund

Exam committee:

Examiner 1: Harry Lankreijer
Department of Physical Geography and Ecosystem Science,
University of Lund

Examiner 2: Jutta Holst
Department of Physical Geography and Ecosystem Science,
University of Lund

Acknowledgments

First of all, I would like to thank Martin Berggren for the chance to do my master thesis in his working group of Aquatic Biogeochemistry. His lectures during my studies stirred my interest in this subject and I am happy that I got the chance to increase my knowledge which has only enhanced my interest in this topic. I appreciate his weekly feedback and him checking up on me and my progress. Even with his busy schedule, he found time to answer my question, give feedback, and provide support. Thank you!

Thank you to the Aquatic Biogeochemistry group who supported and helped me in many ways. It was a very nice routine to start the weekly meetings with a check-up on the owls and see their development from week to week. It provided me with diverse and new input. I enjoyed the Thursday meetings I learned a lot and it helped me to think outside the box and expand my focus beyond my work. Thank you, Hani, for helping me in the laboratory, and Enass for your nice and motivating words. A special thanks goes to Mayra! Without you, I would have never made it to Umeå and enjoyed it as much as I did. I am happy that we had the chance to meet and work together in the laboratory even under pandemic conditions. I learned a lot from you, and I am grateful for all the experiences you have shared with me. Regarding this, I would like to thank Umeå University for giving us the opportunity to use their facilities.

Furthermore, thank you to Harry Lankreijer, for the feedback on my project proposal, half-time report, and the final thesis. The feedback was always helpful and constructive. Also, to Pia, my opponent and fellow student, but most important, friend, for all her feedback during the working process.

Thank you, to the Abisko Scientific Research Station, for providing meteorological data. Also, a thank you to Andreas Persson for providing the samples and the Stordalen catchment map.

Of course, many people helped me on my way, and I want to say thank you to all of them! A big thank you goes to my flatmates and friends who supported me. I greatly enjoyed all the nice and motivating Fikas we had.

Abstract

Climate change-induced thawing of permafrost mobilizes previously frozen carbon of high potential reactivity, thereby, fuelling microbiological production of greenhouse gases. For this work, an analysis of the quantity, quality, and bioreactivity of DOC in streams from the Stordalen discontinuous permafrost catchment was carried out with stream water samples during the relatively warm summer of 2018.

In the study area permafrost is limited to peatland which is present in lowland areas. We hypothesized that (*i)* peatland-influenced streams have a higher dissolved organic carbon (DOC) concentration than streams in upland areas of the Stordalen catchment. However, no strong differences in the quantity of DOC between peaty lowland and well-drained upland areas were found. In general, DOC quantity was lower compared to levels obtained by previous studies conducted in the area but due to the lack of discharge measurements for this study, a comparison with other studies is difficult. Furthermore, no clear pattern was detected regarding the extent of carbon degradation, represented by a small range of the ratio between the isotopically stable carbon-12 and carbon-13. However, a slightly enhanced degradation in areas located in upland areas was detected.

Additionally, it was predicted that (*ii)* DOC from upland areas was associated with low molecular weight and relatively high bioreactivity compared to DOC derived from peaty lowland areas. The DOC from all sampled sub-catchments, including the lowland sampling points in the peat, showed surprisingly high bioreactivity, although the upland catchments, where peat was not present, were generally associated with the lowest molecular weights and highest bioreactivity of the DOC.

Upland areas are characterised by a faster turnover of carbon, as oxygen can diffuse into the shallow organic layer. Thus, *(iii)* the share of labile C was higher in better-drained upland areas than in peatland areas. This work showed how quantifiable amounts of low molecular weight DOC can reach streams from permafrost catchments during a warm and dry summer, due to the increasing thickness of the active layer.

Keywords: *Physical geography, ecosystem analysis, permafrost degradation, DOC, DOC concentration, stable isotope carbon signature, DOC quality, DOC degradation*

Table of Contents

List of Figures

List of Tables

List of Abbreviations

cal. BP	Calibrated year before present
C	Carbon
°C	Degree celsius
CH_4	Methane
CO_2	Carbon dioxide
e.g.	Exempli gratia
DO	Dissolved oxygen
DOC	Dissolved organic carbon
h	Hour
HCl	Hydrochloric acid
L	Litre
m	Meter
m.a.s.l.	Meter above sea level
mL	Millilitre
NaOH	Natriumhydroxid
OC	Organic carbon
OM	Organic matter
O_2	Oxygen
Pg	Petagrams
RQ	Respiration quotient
UV	Ultraviolet light
SDR	Sensor Dish Reader
SOC	Soil organic carbon
α	Significance level
µm	Micrometre
µL	Microliter
%	Percent
^{13}C	Carbon 13 isotope (stable isotope)
^{12}C	Carbon 12 isotope (stable isotope)
$\delta^{13}C$	Isotopic signatures of the ration $^{13}C/^{12}C$

Introduction

Increasing air temperatures in higher latitudes lead to the degradation of permafrost, which is defined as frozen ground with a temperature of or below 0°C for at least two consecutive years (IPCC 2013; Schuur et al. 2008; Strand et al. 2020). Climate change-induced thickening of the active layer, the layer above the permafrost which is undergoing an annual thawing and refreezing cycle, mobilizes previously frozen, and thus unavailable, organic carbon with high potential reactivity (Schuur et al. 2008). Therefore, permafrost degradation can alter the dynamics of dissolved organic carbon (DOC), causing a change in the downstream aquatic carbon (C) cycle (Olefeldt and Roulet 2014).

The properties of DOC depend first on the catchment characteristics from which it is derived, and second on the source of stream water (Sebestyen et al. 2021). In peatland, underlain by permafrost, the DOC discharge is confined to the upper layer of the soil profile (the active layer). The permafrost can serve as a barrier for vertical water movement (Carey 2003; Olefeldt and Roulet 2014).

Landscape topography leads to highly heterogeneous catchment characteristics. While in lowlands, water accumulates and leads to peat-forming soil conditions, soils in uplands are well-drained, allowing aerobic C decomposition (Quinton and Marsh 1999; Schlesinger and Bernhardt 2013). These differences affect the extent of C degradation and thus, the biolability of the C (Fellman et al. 2008; Xenopoulos et al. 2021). The soil of peatland is water-saturated, which causes a lack of oxygen, resulting in a reduced decomposition of organic matter (OM) and its accumulation over decadal to millennial timescales (Schlesinger and Bernhardt 2013). Further, cold temperatures impede decomposition in permafrost regions (Ewing et al. 2015). Thus, DOC originated from peatland is derived from poorly decomposed OM (Olefeldt et al. 2013; Sebestyen et al. 2021). On the contrary, aerobic decomposition in well-drained upland regions leads to a DOC export that is characterized by freshly dissolved matter (Schlesinger and Bernhardt 2013; Sebestyen et al. 2021).

However, due to a thickening of the active layer, OM from further down in the peat soil profile becomes accessible for degradation (Schuur et al. 2008). This OM was degraded due to anaerobic decomposition by anaerobiosis. Furthermore, OM was degraded during soil formation processes. Both results in highly biolabile C (Mu et al. 2014; Ewing et al. 2015).

Most studies carried out in higher latitudes focus on the land-atmosphere C exchange on terrestrial systems, while only a little research is directed at the lateral loss of C

(Lundin et al. 2013). A less investigated but very important area of research is the lateral transport of DOC in northern latitudes, as this plays a crucial role in the global C cycle (Hinzman et al. 2005; Olefeldt et al. 2013; Mzobe et al. 2020). As lateral transport is influenced by the surrounding landscape, it is of great interest to understand its influence on DOC contained in inland waters (Mzobe et al. 2018). In addition, the relationship between DOC composition and bioavailability should be further investigated, particularly in relation to permafrost thaw (Olefeldt et al. 2013). It is important to fill the knowledge gap since the impact of peatlands in subarctic catchments hosting permafrost is relevant as permafrost thaw affects solutes discharge from land into streams and rivers (Zhao et al. 2021). This is especially urgent since climate predictions for higher latitudes indicate an increase in annual mean temperature as well as an increase in precipitation, both accelerating permafrost degradation (IPCC 2013), which can already be observed (Strand et al. 2020). With an expanding depth of the active layer, it is of increasing importance to understand how the biodegradation of organic carbon may be affected (Heslop et al. 2019). As permafrost degradation is associated with impacts on permafrost-carbon feedback, it is highly relevant to contribute knowledge in this area and gain greater understanding of the situation at hand.

The goal of this work is to improve the knowledge of stream DOC properties and thus understand the link between the bioavailability of DOC in relation to its properties in the discontinuous permafrost region of Abisko, northern Sweden. This is seen in context to the spatial origin of DOC in the Stordalen catchment (upland areas vs. peaty lowlands). The Stordalen catchment is characterised by peatland in the lower elevated regions, which contain permafrost, while birch forest and tundra areas are the dominant features in the upland regions (Olefeldt et al. 2013).

The following research questions will be addressed:

(I) Is the DOC concentration in peat-influenced streams higher than in upland-influenced streams?

(II) Is DOC originated from peat-influenced streams less bioreactive (molecular weight) compared to upland originated DOC?

(III) Regarding the lability classes of the DOC exported in the Stordalen catchment: Is the share of biolabile DOC (of total DOC) higher in upland areas than in peaty lowlands and, vice versa, the share of recalcitrant DOC higher in the peaty lowland areas?

To test these research questions, statistical approaches were applied and if a certain correlation was detected, the hypothesis was supported.

We hypothesized that DOC originated from peatlands enters streams relatively undiluted, and shows a higher concentration than DOC derived from upland regions. This is, for example, due to the longer residence time of water in peaty lowlands. Peat has a high water-holding capacity and a thick organic layer, 1-2 m at the Stordalen catchment (Olefeldt and Roulet 2014; Quinton and Marsh 1999; Olefeldt 2011). However, in upland regions, only a shallow organic layer over a mineral layer occurs (Fellman et al. 2008). This difference in the OM pool combined with the flushing out of water in upland regions due to the steeper slope also causes these differences in DOC concentrations (Hobbie et al. 2000; Olefeldt 2011). Moreover, the discharge in the upland areas is dominated by subsurface runoff. Since mineral soil is commonly present there, DOC is absorbed by soil minerals as it flows through the catchment (Sebestyen et al. 2021). As OM decomposition rate is higher in well-drained upland areas than in peatland, it can be expected that the isotopically lighter ^{12}C has already been utilized by decomposition processes, therefore, creating an enrichment of the isotopically heavier ^{13}C in upland areas (Lambert et al. 2014). However, C further down in the peatland soil profile has been exposed to enhanced decomposition (Mu et al. 2014; Ewing et al. 2015). Therefore, the C isotope depth profile may show a similar pattern to the one in upland areas (Lambert et al. 2014). Also, a difference in the molecular structure of the DOC derived from uplands and peaty lowlands is expected. Likewise, due to the different degradation rates between the two regions, it is assumed that DOC discharged from higher elevated regions has protein-like, low-molecules weight, while peat-derived DOC is characterized by high-weight, humic-like molecules with an aromatic structure and lower biodegradation (Xenopoulos et al. 2021). However, freshly thawed ancient C is rapidly mineralized due to its low-molecular weight organic acids (Drake et al. 2015). Therefore, thickening of the active layer may influence the results and therefore extend the source of C with different traits (Drake et al. 2015).

To test the hypotheses, an experimental approach was conducted: Water samples were collected at several sampling points distributed in the Stordalen catchment in the summer of 2018, both in the uplands and in the lowlands. With four analysis experiments (DOC concentration, stable C isotopic composition, quality characterization, and biodegradation of the DOC) DOC characteristics were assessed, and samples were compared regarding their origin (lowlands vs. uplands).

1 Background

Dominating landscape elements in the northern, boreal regions are commonly characterized by peatland in lowland areas and forested upland areas with mineral soil (Köhler et al. 2008; Sebestyen et al. 2021). In peatlands in these regions, the presence of permafrost is a common feature (Tarnocai et al. 2009), therefore permafrost degradation can alter peatland-derived DOC (Olefeldt and Roulet 2012). Furthermore, peatlands are characterized by a high soil organic carbon (SOC) content, which makes them highly relevant regarding the global carbon (C) cycle (Tarnocai et al. 2009). In the study area, the presence of permafrost is confined to peatlands (Olefeldt et al. 2013).

1.1 Permafrost

Permafrost is a widespread phenomenon in the Arctic and boreal regions of the Northern Hemisphere, covering 24% of the exposed land surface (Zhang et al. 2003; Schuur et al. 2008). It occurs in regions with a cold climate and weather (IPCC - Intergovernmental Panel on Climate Change 2013), such as higher latitudes and high mountainous regions (Schuur et al. 2008). This work focuses on landscapes within the terrestrial permafrost in higher latitudes. Permafrost is characterized by frozen subsurface materials at a ground temperature of or below 0°C for at least two consecutive years (IPCC 2013). Over the range from decades to millennia, and especially during interglacial periods, organic matter (OM) has accumulated in the northern regions, forming a large C sink. A change in climate towards colder conditions caused a deceleration in the decomposition of OM, resulting in a vast C pool (Schuur et al. 2008). Permafrost, therefore, has an important influence on the global C cycle and thus on the global climate. Tarnocai et al. (2009) estimated that the amount of stored C in all northern circumpolar permafrost regions combined is about 1672 PgC, representing 50% of global belowground organic carbon (OC).

Permafrost is highly sensitive to changes in climate (Schuur et al. 2008; IPCC 2013). With an increase in temperature, the previously frozen and thus unavailable OC becomes bioavailable due to thawing. Microorganisms metabolize this OC, which leads to emissions of greenhouse gases, such as carbon dioxide ($CO_{2)}$ and methane (CH_4), into the atmosphere (Schuur et al. 2008). Therefore, permafrost is not only vulnerable to climate change but also amplifies it (Biskaborn et al. 2019).

Permafrost can be divided into different zones depending on the extent of the area underlain by permafrost. Areas underlain to 90-100% by permafrost are classified as continuous permafrost and to 50-90% as discontinuous permafrost. If less than 50% is underlain by permafrost, it is defined as sporadic permafrost (Johansson et al. 2006). The area underlain by permafrost decreases from north to south in the arctic and

subarctic region (Schuur et al. 2008). The thickness of continuous permafrost can reach multiple hundred meters. Southwards, it is replaced by discontinuous permafrost, which is intercepted by unfrozen areas but shows a regular distribution pattern (King 1986). The unfrozen areas are determined by ecological parameters such as topography, snow cover, vegetation, and hydrology (King 1986; Schuur et al. 2008). The thickness of the permafrost decreases from continuous to discontinuous permafrost, while the thickness of the active layer increases (King 1986). Sporadic permafrost occurs at permafrost favourable conditions (cold climate and weather) but does not show a regular pattern (King 1986).

Throughout the year, the upper layer in all types of permafrost regions undergoes thawing and freezing processes due to seasonal temperature changes. The layer at the surface, called the active layer, thaws when temperatures increase during the summer and refreezes when temperatures drop in autumn (Schuur et al. 2008). The depth of the active layer is thinnest in continuous permafrost regions, only a few centimetres, and growing deeper towards discontinuous and sporadic permafrost regions, where it can reach a depth of several meters (Schuur et al. 2008). The active layer represents the layer above the permafrost in which biological activity such as microbial decomposition and plant root functions take place. The layer below, the actual permafrost, contains frozen and thus unavailable OM which stores a large amount of C (Schuur et al. 2015; Johansson et al. 2006). The active layer thickness varies between years and is determined by different factors, such as air temperature, vegetation cover, drainage, soil type, moisture content, snow cover, topography, and precipitation (Harris et al. 1988; Johansson et al. 2006).

Nowadays, permafrost degradation is noticeable in nearly all permafrost regions, reaching from continuous, to discontinuous or sporadic permafrost (IPCC 2013). It can be expected that with continuing warming of the northern regions, the discontinuous and sporadic permafrost distribution will be shifted polewards (Romanovsky et al. 2019).

1.2 Permafrost degradation

Increasing permafrost temperatures and thickening of the active layer are the two main factors of permafrost degradation (Zhao et al. 2021), leading to reduced permafrost extent, which can result in the disappearance of permafrost (Harris et al. 1988).

Strand et al. (2020) observed that the active layer thickness increased across the Arctic since the 1990s, reaching a maximum during 2016-2018. An increase in permafrost temperature since the 1980s, especially in permafrost areas located in higher latitudes, has been recorded as well (Romanovsky et al. 2019; IPCC 2013; Biskaborn et al. 2019).

This is in line with the rising surface air temperature in the European Arctic over the past 40 years with 2016 as the warmest year on record (1979-2018) and 2018 as the second warmest year (2°C above average) (European Arctic | Copernicus 2021 - assessed February 2021).

Regions having a mean annual air temperature of around 0°C are especially vulnerable to a warmer climate as a small increase in temperature can result in a change of the freezing state (Johansson et al. 2006). It is assumed, that permafrost in these regions disappears first and observations show that permafrost degradation is already happening in the regions around Abisko (Johansson et al. 2006).

1.3 Permafrost at the study area

Abisko is located in discontinuous and sporadic permafrost zones in northern Sweden and holds permafrost in peatlands (Strand et al. 2020). Peat formation occurs when the decaying litter is incorporated into the anaerobic soil layer where the decomposition rate is reduced. As a consequence, the input of C by litter is greater than the loss. C loss is caused by its degradation to CO_2 and CH_4 as well as due to runoff including DOC (Clymo 1984; Malmer et al. 2005). This imbalance between OM input and decomposition leads to the accumulation of soil OM. Over time the soil OM becomes buried and compacted under a layer of newly deposited plant detritus (Schlesinger and Bernhardt 2013). The *Sphagnum* mosses, which are a dominant species in northern peatlands, contribute to peat formation as their litter is recalcitrant (Malmer et al. 2005). The accumulation of OM over the last 5000 cal. BP years (Malmer et al. 2005) formed a peat layer that is 1-2 m thick at the study area (Olefeldt and Roulet 2014).

Peatlands are common in all permafrost zones and store globally up to 277.3 Pg C (Tarnocai et al. 2009). In the study area, the soil type and the amount of OM it contains determine the restriction of permafrost occurrence to peatland. With an increase of OM in the soil, the water storage capacity increases, and thus heat penetrates more slowly into deeper layers than it does in sandy soil (Quinton and Marsh 1999; Smith and Riseborough 2002). Therefore organic-rich soil, such as peat, is more favourable to contain permafrost (Johansson et al. 2006). Smith and Riseborough (2002) showed that permafrost is absent in mineral soils with a mean annual air temperature of above -2 °C, while in organic soil, permafrost can occur by a mean annual air temperature of 1-1.5 °C. Abisko has a mean air temperature of 0.0 +/- 0.9 °C (1980-2009) (Olefeldt and Roulet 2014). Accordingly, the soil conditions in the upland regions of the study area, which are not favourable for peat and with that, permafrost formation, may be the reason for the absence of permafrost. The occurring soil is well-drained and less developed, characterised by shallow to moderately deep O (organic) horizons above a mineral soil (Fellman et al. 2008; Olefeldt et al. 2013; Olefeldt and Roulet 2014). This

results in a low abundance of peat with outcrop and steep slopes in the upland region of the study area (Mzobe et al. 2018 and 2020).

1.4 Permafrost degradation at the study site

As the mean annual air temperature has been increasing in Abisko since 1978, the permafrost degradation in this area is visible and linked to a thickening of the active layer (Strand et al. 2020). For the study areas Heliport and Storflaket, both located in the region around Abisko, the active layer thickness increased by 17 and 6 cm respectively, over the observed period (2000-2018) (Strand et al. 2020). Climate projections for Abisko predict an increase in both mean annual air temperature and precipitation (IPCC 2013). The increase in precipitation is expected to predominantly occur in autumn/winter and thus the snow cover will become thicker (Johansson et al. 2006). With increasing snow cover depth less heat can be released from the ground due to the thermal isolation of snow (Zhao et al. 2021). Åkerman and Johansson (2008) found a positive correlation between increased thawing of the active layer and snow depth, for five out of nine sites tested in northern Sweden (Torneträsk including Abisko). Furthermore, mean summer air temperature, as well as thawing degree days, are positively related to active layer thickness which both also showed an increase (Åkerman and Johansson 2008; Strand et al. 2020).

1.5 Consequences of permafrost degradation

As the active layer deepens, the previously frozen OM becomes mobilized and provides an additional source pool of OC (Spencer et al. 2015). The mobilized soil OC can be released after decomposition as gas to the atmosphere or through leaching to watercourse (Clymo 1984). The transport of terrestrially-derived C into inland waters is described as lateral C flux (Drake et al. 2018) and determines the transportation of C within the aquatic system (Cole et al. 2007). Processes like C storage in sediments, C exchange (outgassing of CO_2) with the atmosphere, and transport occur along the way (Cole et al. 2007). Therefore, aquatic systems play an important role in the global C cycle. There is evidence that nearly half of the terrestrial-driven C which enters inland aquatic systems gets buried in aquatic sediments or emitted into the atmosphere while the remaining C is transported to the ocean (Cole et al. 2007). The main form in which C occurs in rivers is as DOC (Hope et al. 1994).

DOC is the C portion of dissolved organic matter (DOM) which has a terrestrial or aquatic source and originates from the mineralisation of OM or directly from root excretions (Carey 2003; Fellman et al. 2008). DOC, as well as DOM, is described by its particle size, which includes particles that pass through a 0.45-µm filter (Hope et al. 1994).

1.6 Consequences for the ecosystem

An increased amount of terrestrial-driven C entering inland aquatic systems has been noticed in different landscapes, including permafrost areas, resulting in a browning of the inland water (Lapierre et al. 2013; Wauthy and Rautio 2020). This brownification has consequences for the ecosystem as less light can penetrate through the water column. This results in a reduced primary production with consequences for higher levels in the food web as food availability decreases (Feuchtmayr et al. 2019; Wauthy and Rautio 2020). In addition, OM absorbs light, resulting in more solar energy being trapped closer to the water surface, and thus, reducing the depth of the epilimnion (Feuchtmayr et al. 2019; Strock et al. 2017). Epilimnion refers to the warmer and therefore lower density surface layer in the water column of a stratified lake (Schlesinger and Bernhardt 2013). With a decreasing thickness of the epilimnion, available resources for the phytoplankton production, which takes place there, also decreases, with possible consequences for higher tropical levels (Strock et al. 2017). The addition of OC also provides an increasing source of energy for bacterial respiration, increasing their biomass and shifting freshwaters toward a heterotrophic system (Wauthy and Rautio 2020). Consequently, a positive correlation between the DOC concentration and the CO_2 flux in boreal lakes has been observed (Jonsson et al. 2003; Lapierre et al. 2013).

1.7 Terrestrial-derived DOC export from lowlands and uplands

DOC accumulates in inland water either by overland or subsurface flow as the stream flows through the catchment. Hence, the catchment characteristics, as well as the sources of stream water, determine the trait of DOC (Sebestyen et al. 2021).

In permafrost regions, DOC discharge into streams primarily originates from overland flow or near-surface subsurface flow as the frozen ground forms a barrier (Carey 2003). In the study area, where permafrost only occurs in lower laying peatlands, the discharge from these regions is confined to the upper organic soil layer. Furthermore, the low mineral content in peat layers prevents contact between DOC and mineral soil, which absorbs DOC at its surface (Olefeldt and Roulet 2014; Sebestyen et al. 2021). However, upland catchments in the study area are dominated by mineral soils, and especially during summer the water table falls into it (Quinton and Marsh 1999; Fellman et al. 2008; Sebestyen et al. 2021). Thus, in these regions, water penetrates deeper into the mineral soil, causing the dominant discharge to be subsurface flow. Consequently, more interaction between DOC and the mineral surface occurs (Quinton and Marsh 1999; Carey 2003). In tundra regions the productivity of biomass is low, resulting in a thin soil layer and therefore small terrestrial DOC sources (Ma et al. 2019).

Well-drained soil allows oxygen to diffuse deeper into the soil and thus aerobic decomposition can take place, which results in a faster turnover time of C than in water-saturated soils (Schlesinger and Bernhardt 2013; Lambert et al. 2014). The recently solved DOM exported from upland catchments is originated by leaves, roots, or OM residuals (Sebestyen et al. 2021). On the contrary, the water table in peatland is with seasonal fluctuations within the thick organic layer, causing water-saturated peat and anaerobic decomposition (Schlesinger and Bernhardt 2013). This leads to a prolonged turnover of C and thus an accumulation of OM (Morris and Waddington 2011; Schlesinger and Bernhardt 2013; Ewing et al. 2015). Exported DOC from these poorly decomposed OM is thus derived from young generated to centuries-old peat (Sebestyen et al. 2021). In permafrost regions, low temperatures reduce the microbial degradation of OM as well (Ewing et al. 2015).

1.7.1 DOC concentration

According to Mu et al. (2014), DOC concentration in soil decreases from a humic horizon towards the sedimentary bedrock. The thickness of the humic horizon varies and determines the DOC source pool. Upland areas are often characterized by a shallower organic layer over a mineral layer and thus more absorption of DOC on the mineral surface (Carey 2003; Fellman et al. 2008; Sebestyen et al. 2021). Interchangeable processes that occur besides absorption of C on the mineral soil are desorption, complexation, and precipitation (Reddy et al. 1997). These processes are depending for example on the pH of soil and with increased alkalinity more DOC mineral association occurs (Tavakkoli et al. 2015). Furthermore, the residence time of the pore water is critical for the DOC concentration, as a longer residence time causes an accumulation of DOC compounds (Olefeldt 2011). Peatlands are characterised by a higher water storage capacity than mineral soils, therefore, the residence time of soil water in peatlands is longer than it is in mineral soils (Olefeldt 2011).

The concentration of DOC is influenced by annual changes (Olefeldt et al. 2013). For example, during storm events or snowmelt, perennial runoff from the surrounded upland areas further dilutes the runoff in lower areas (Köhler et al. 2008; Sebestyen et al. 2021). In upland catchments, especially in tundra regions, streams are fed by precipitation and snowmelt (Mzobe et al. 2018), with a low DOC concentration (Ma et al. 2019).

Likewise, temperature affects the release of DOC into streams, as soil OM decomposition increases with warmer temperatures (Grieve 1991). As temperature is a limiting factor for C mineralization, an increase towards summer induces an increase in provided DOC (Grieve 1991). Furthermore, warmer temperatures include a thawing

of the active layer in peatlands and thus an extended C pool (Grieve 1991; Köhler et al. 2008; Heslop et al. 2019).

1.7.2 DOC stable carbon isotope signature

Spatial variation also occurs in the isotope composition of the C regarding the environment of origin. The stable isotopes of C are ^{12}C and ^{13}C. Their ratio $^{13}C/^{12}C$ is given as $\delta^{13}C$ value and expresses the extent of degradation (Beaupré 2015).

The calculation of the $\delta^{13}C$ value is based on a standard $^{13}C/^{12}C$ ratio, where a smaller $\delta^{13}C$ value represents isotopically lighter OC with more ^{12}C, while a higher $\delta^{13}C$ value represents isotopically heavier OC with more ^{13}C (O'Leary 1988). The ^{13}C isotope has a higher mass due to the additional neutron, therefore, its breakdown needs more energy than for the breakdown of ^{12}C. The energy costs for a physical transformation are thus higher if the molecule contains ^{13}C (Beaupré 2015). Hence, decomposers preferably utilize the isotopically lighter ^{12}C in decomposition processes, causing a relative enrichment in ^{13}C in the remaining OM (Mu et al. 2014). Thus, the stable C isotope composition indicates how well the OM has been degraded, as there is less ^{12}C left when degradation is enhanced (Lambert et al. 2014; Beaupré 2015).

According to Lambert et al. (2014), not only the presence of oxygen and thus aerobic or anaerobic degradation influence the differences in C isotope composition. Also, differences can occur within the soil profile, as higher $\delta^{13}C$ values have been also observed in deeper soil layers. With increasing soil depth, the extent of the decomposition of the OC increases, represented by an enrichment of ^{13}C (Mu et al. 2014). The distribution of the isotopically heavier C isotope further down in the soil profile indicates that during the soil formation process the labile C has been utilized (Mu et al. 2014). Furthermore, clay minerals, occurring mainly below the organic layer, absorb ^{13}C-enriched components, resulting in a greater $\delta^{13}C$ with depth (Wynn et al. 2005).

1.7.3 DOC optical characterization

Optical molecular differences are also evident in the structure of DOC depending on its environment (Fellman et al. 2008). DOC consists of heterogeneous chemical compounds with varying lability depending on the degradation and transformation of OM, defined by its molecular weight (Vitale and Di Guardo 2019). It ranges from low-molecular weight compounds (e.g. carbohydrates, carboxylic acids, and amino acids) to complex high-molecular weight DOC such as fulvic and humic acids (Aitkenhead-Peterson et al. 2003). High-molecular weight compounds have a complex structure of fused aromatic rings (Kanaly and Harayama 2000). Bacteria must exceed the stabilising resonance energy of the fused aromatic compounds in order to use the C as an energy

source (Fuchs et al. 2011). With an increasing number of aromatic rings the electrochemical stability of a molecule increases (Kanaly and Harayama 2000). In the presence of oxygen, the aromatic structure is catalysed by oxidation (Kanaly and Harayama 2000). Oxygen serves as an electron acceptor to clave the aromatic structure (Fuchs et al. 2011). In lack of oxygen, an alternative electron acceptor serves, however, the energy yield is lower (Fuchs et al. 2011). Thus, in the absence of oxygen, an accumulation of OM and hence aromatic DOC due to a reduced degradation occurs (Schlesinger and Bernhardt 2013).

Continuous degradation of DOC into smaller molecules is processed with age and results in low-molecular weight compounds, which are metabolically labile (Beaupré 2015). Less degraded DOC is characterised by higher molecular weight and an aromatic structure (Xenopoulos et al. 2021). Aromatic C compounds are negatively correlated with bioavailable DOC (Fellman et al. 2008). Hence, low-molecular weight DOC is determined to be high-quality. It consists of protein-like compounds that are highly biolabile due to their energetically beneficial state (Fellman et al. 2008; Ewing et al. 2015).

The quality of DOC does not only depend on its degradation state, it is further determined by litter input, root exudates, animal residues, and throughfall (Van Hees et al. 2005; Vitale and Di Guardo 2019). Throughfall is the wash-off of deposition on leaves and branches of a tree caused by rainfall onto trees (Van Stan and Stubbins 2018).

Only a small fraction of the total DOC is determined as low-molecular weight, approximately 20% (Aitkenhead-Peterson et al. 2003). This is enhanced, by the short residence time in soil of low-molecular weight organic compounds compare to high-molecular weight organic compounds. Low-molecular organic compounds are rapidly assimilated by the soil microbial community due to their relatively simple structure (Van Hees et al. 2005).

To measure the molecular size in this work, the light absorption ratio between the wavelength 250 nm and 365 nm was used (a250/a365). With an increase in the molecular size the a250/a365 decreases, as high-molecular weight DOC has an enhanced light absorption at longer wavelengths (John et al. 2008). Thus, a lower a250/a365 indicates a higher average molecular weight and more aromatic molecular structure (Peuravuori and Pihlaja 1997; Yang and Xing 2009).

The optical characteristic of DOC shows a similar spatial pattern as the C isotope signature. Due to enhanced degradation of OM in the presence of oxygen, DOC from

these areas has a lower molecular weight. DOC from areas with a lower degradation rate, in contrast, shows higher aromaticity and thus higher molecular weight (Olefeldt et al. 2013). However, with an increase of the active layer thickness, the ancient, freshly thawed, permafrost-derived DOC is rapidly mineralized by microbial decomposition due to its low-molecular weight (Drake et al. 2015). Selvam et al. (2017) also describe higher biodegradation of DOC from freshly thawed permafrost layer than from the active layer, since molecules in the active layer have a higher molecular weight, represented by humic-like components. The increasing biolability of C within the soil profile is attributed to long-term anaerobiosis in C-rich and oxygen-low environments over millennia (Ewing et al. 2015). Therefore, the abundance of low-molecular weight DOC increases with soil depth and is not limited to the presence of oxygen.

1.7.4 DOC biodegradation

The biolability of DOC depends on both its chemical character and its physical environment (Ewing et al. 2015). In both landscapes, forested uplands and peaty lowlands, bacteria use OC as an energy source (Berggren et al. 2007). Thereby C can be classified according to its lability. Labile C means that it is highly degradable through abiotic and biotic transformations and is the opposite of recalcitrant C, which is not readily degradable (Xenopoulos et al. 2021). If DOC is biolabile, it means it can be degraded by microorganisms (Xenopoulos et al. 2021).

2 Materials and Methods

2.1 Study site description

Stordalen catchment (68°21`N, 19°03`E) is located 10 km east of Abisko in the Torneträsk region in northern Sweden and drains into the Torneträsk lake (Olefeldt and Roulet 2012; Mzobe et al. 2018). The region around Abisko, in the subarctic climate zone, is represented by discontinuous and sporadic permafrost zones, with discontinuous permafrost in mountainous regions 800-1000 meter above sea level (m.a.s.l.) and sporadic permafrost in peaty mires in lowland areas (Mzobe et al. 2020; Strand et al. 2020). The Stordalen catchment is characterized by sporadic permafrost and has a size of 14.5 km^2 (Figure 1). Its elevation ranges from ~ 800 m.a.s.l. in the south to ~360 m.a.s.l. in the north (Mzobe et al. 2018 and 2020). The catchment is determined by a break in slope which divides it into a mountainous region, in the south and a flatter peatland region further north (Olefeldt and Roulet 2014). For this work, nine sampling points (monitoring points) defined by Olefeldt et al. (2013) were used (Figure 1). Each presents a sub-catchment (A1-A7 and B1/B2), within the Stordalen catchment with different landscape compositions (Olefeldt et al. 2013). These sub-catchments were defined based on the sampling points from Olefeldt et al. (2013).

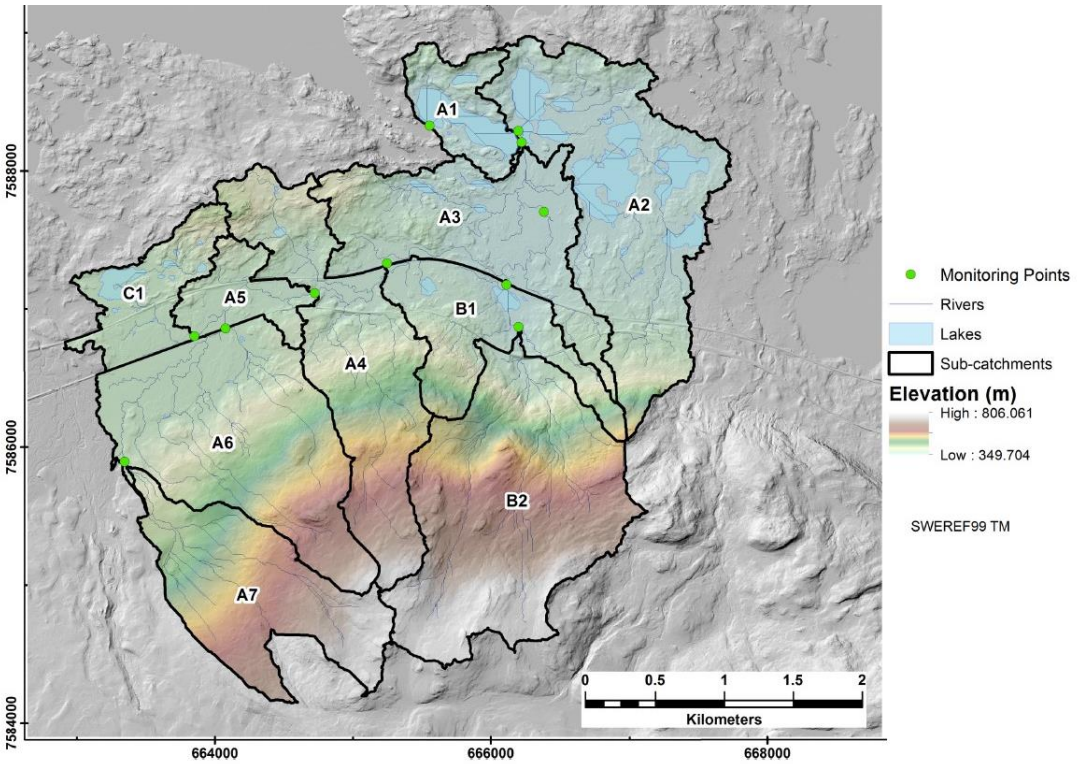

Figure 1. *Map of the Stordalen catchment (Torneträsk region) with the sub-catchments (A1-A7 and B1/B2). This map is provided by the study from Mzobe et al. (2018). Approval was obtained from Pearl Mzobes and Andreas Persson.*

2.2 Sub-catchment description

An overview of the different morphometric parameters and the peatland cover for each sub-catchment is given in Table 1 and is supported by Figure 1. The morphological parameters mean elevation, relief, average slope, catchment area, and peatland cover were chosen. These parameters were selected to present the diversity of the different sub-catchments and are parameters that define upland areas and peaty lowlands. The mean elevation represents the averaged elevation of the defined sub-catchment in m.a.s.l. Relief [m] is the difference between the highest and lowest elevated point of a sub-catchment. With the average slope, the mean of all measured slope angles within the sub-catchment is presented in degrees. The sub-catchment area expresses the area of each sub-catchment in km^2 (Mzobe et al. 2020). These parameters were explained and taken from the study by Mzobe et al. (2020), which used a (digital elevation model) DEM with a 2 m resolution. Peatland cover expresses how much of each sub-catchment [%] is covered with peat relative to the entire Stordalen catchment and was taken from the study by Olefeldt et al. (2013).

Table 1*. Characteristics of each sub-catchment of the Stordalen catchment including mean elevation, relief, average slope, area, soil, and landcover of each sub-catchment (A1-A7, B1/B2). Data elevation, relief, average slope, and catchment area are from Mzobe et al. (2020), while information about soil/landcover is additionally combined with Mzobe et al. (2018) and Olefeldt et al. (2013). Percentage data of sub-catchment covered by peatland are taken from Olefeldt et al. (2013).*

Sub-catchment	Mean elevation [m.a.s.l.]	Relief [m]	Average slope [degrees]	Sub-catchment area [km^2]	Peatland cover [%]
A1	360.59	45.41	8.65	0.49	6.4
A2	365.30	203.43	5.81	2.34	6.5
A3	367.51	146.36	6.41	1.57	4.7
A4	472.01	384.50	10.16	1.81	6.4
A5	386.70	44.22	5.95	0.44	7.2
A6	457.93	373.12	8.89	2.17	6.1
A7	581.15	394.92	11.39	1.45	0.6
B1	396.89	201.86	9.59	0.95	0.1
B2	610.02	453.91	14.17	2.61	0.0

Through the Stordalen catchment runs both a road and rails. These cross the catchment from west to east and pass between the sub-catchments C1/A5 and A6 as well as B1 and A3. Their parallel course is marked by the straight line dividing these sub-catchments. Other sub-catchments are not limited by it. The sample points are presented by the green points in the map (Figure 1) and located at the outflow of each sub-

catchment (Olefeldt et al. 2013). For the analysis of this work, the individual sub-catchment characteristics have been considered and not the upstream characteristics. Even though the stream water was flowing through the Stordalen catchment before reaching sub-catchments located further upstream in the lowlands, this study assumed that the closed surrounding of the sampling point has the strongest influence on the characteristics of the DOC and did not take the upstream characteristic into account. However, all sub-catchments are nested as they are hydrologically connected. The main stream flows through catchments A1-A7 and the tributary that enters into the main stream flows through sub-catchments B1 and B2 (Olefeldt et al. 2013). Stream water from the sub-catchment A7 flows through all sub-catchments until finally reaches A1, while stream water from the sub-catchments B2 enters into B1 and then into the main stream in sub-catchment A3 where the water becomes further transported through A2 until it reaches sub-catchment A1. Thus, the water in each sub-catchment is influenced by the previous upstream sub-catchments as well. Unfortunately, upstream values were not available for this work and therefore only the single sub-catchment characteristics were assumed to have an influence on the traits of DOC at the sample point.

The following description of the sub-catchments proceeds from south to north and thus from higher elevated regions to lower regions, Table 1 and Figure 1 serve as references. Sub-catchment B2 is the largest sub-catchment and is nearly entirely confined to mountainous regions, represented by the highest mean elevation (610.02 m.a.s.l.) compared to the other sub-catchments of the Stordalen catchment. It is also the sub-catchment with the steepest average slope and relief. Sub-catchment A7 shows a similar trend within a smaller sub-catchment area. The sub-catchment A6 also has some parts located in upland regions, while others are located further down. However, the average slope of this sub-catchment is not as high as the aforementioned sub-catchments since the area located in lowlands is larger. The sub-catchment A4, which is also partially located in the mountainous region, has the third-highest slope and relief, as it extends on a comparably narrow but elongated shape from the mountainous region in the south down to the lowland. Sub-catchment B1 is placed in the transition area from uplands to lowlands, thus a steeper slope (9.59 °). Sub-catchment A5, in the lower elevated areas, shows some forested cover (birch) areas (Mzobe et al. 2018). The second-largest sub-catchment, A2, is mainly located in a lower elevated area. Furthermore, this sub-catchment has the lowest slope (5.81 °). Sub-catchment A1 and A3 show a similar elevation to A2 and belong to the sub-catchments with the lowest slopes.

The cover of peatland is higher in lowland sub-catchments than in upland sub-catchments (Table 1). The proportion of peatland is highest in sub-catchment A5, while the sub-catchments with a peatland cover of below 1% are A7, B1, and B2 (Olefeldt et

al. 2013). The sub-catchment B2 does not contain any peatland. According to Mzobe et al. (2018) areas characterized by tundra and steeper slopes are not dominated by mires. Therefore, sub-catchments located in lower land contain more peatland and thus permafrost is present mainly in lower land.

The upper areas of the Stordalen catchment are characterized by rock outcrops, tundra heath, and only a low abundance of peat. This is particularly true for the sub-catchment B2 and A7 (Mzobe et al. 2018). Mountain birch (*Betula pubescens* ssp. *Czerepanovii*) on less developed soil is the major land class type in the Stordalen catchment (Olefeldt and Roulet 2014). In peaty lowlands, however, the dominating vegetation is the moss *Sphagnum* spp. (Tang et al. 2015; Olefeldt and Roulet 2014).

The description of the landscape is based on previous studies and may have changed since then. The study by Olefeldt et al. (2013) was done in 2007-2009 and Mzobe et al. (2018 and 2020) is using these monitoring points within the sub-catchments defined by Olefeldt et al. (2013).

2.3 Climate summary for the Abisko region

Used temperature data in this section were measured at the Abisko Scientific Research Station, which is located 10 km west of Stordalen (Abisko Scientific Research Station, 2021; Meteorological data from Abisko Observation, daily mean 1985-01-01 – 2020-12-31). The precipitation data were provided by the SMHI, station number 188800 (Abisko) (SMHI | Nederbördsmänge (dygn): Alla Stationer - assessed June 2021).

2.3.1 Temperature

The long-term daily mean air temperature for Abisko was 0.08 ± 9.16 °C for 1985-2020. The year of sampling (2018) was, as already mentioned in the Background section (section 1.2), the second warmest year on record in the European Arctic (European Arctic | Copernicus 2021 - assessed February 2021). In Abisko, the mean air temperature for the year 2018 was 0.3 ± 9.98 °C. For the sampling month (July and August 2018) the mean daily temperature was 12.6 ± 4.1 °C, which was warmer compared to the long-term (1985-2020) daily air temperature for these two months, 10.9 ± 3.1 °C. Also, as seen in Table 2, the daily mean air temperature for the sampling months in 2018 is slightly higher compared to the corresponding temperature of the surrounding 5 years.

Table 2. *Climate summary from Abisko, including daily mean air temperature from July and August 2015, 2016, 2017, 2018, and 2019. For the same period, precipitation amounts (annual and for the sampling month July & August). Mean and standard deviation of the air temperature were calculated from data reported by the Abisko Scientific Research Station (Abisko Scientific Research Station, 2021; Meteorological data from Abisko Observation, daily mean 1985-01-01 – 2020-12-31), and precipitation data were provided by SMHI (SMHI | Nederbördsmänge (dygn): Alla Stationer - assessed June 2021).*

	2015	**2016**	**2017**	**2018**	**2019**
Daily air temperature [°C]: July & August	11.5 ± 2.0	11.0 ± 3.1	10.6 ± 3.0	**12.6 ± 4.1**	12.2 ± 2.8
Cumulative precipitation [mm]: entire year	446.2	363.4	394.1	**287.0**	399.0
Cumulative precipitation [mm]: July & August	76.3	135.8	186.7	**94.1**	62.1

2.3.2 Precipitation

Long-term cumulative precipitation (1988-2020) for the sampling month (July & August) was 105.33 ± 37.62 mm while for the year 2018 it was 94.1 mm. This shows that the precipitation in July and August 2018, was slightly below the long-term mean. As seen in Table 2, some of the adjacent years also show lower precipitation in these months. But the annual average for the year 2018 shows the lowest cumulative precipitation within these 5 years.

Figure 2 shows the mean cumulative monthly precipitation pattern over the surrounding years of sampling (2015-2020 excluding 2018) and individually the pattern of 2018. It seems that the lower annual precipitation in 2018 (Table 2) is caused by uncommonly low winter and spring precipitation in 2018 (January – May). Also, July and December 2018 had a lower precipitation compared to the surrounding years. In the appendix (Figure AI), an additional daily precipitation pattern only from the sampling month can be found.

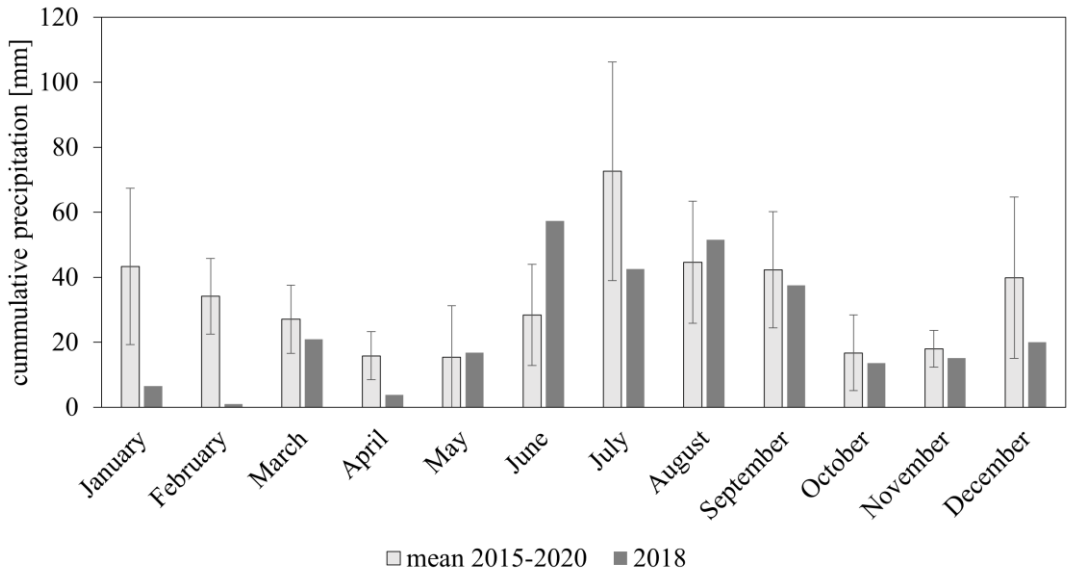

Figure 2. *Abisko precipitation: Light grey columns represent mean cumulative monthly precipitation (mm) from 2015-2020 (excluding 2018) with error bars. Monthly cumulative precipitation for 2018 is shown individually for 2018. On the x-axis the months are presented. 2016 and 2020 were leap years and the precipitation amount for 31-12-2017 is missing. All other daily precipitation values were given and taken from SMHI (SMHI | Nederbördsmänge (dygn): Alla Stationer - assessed June 2021).*

2.4 Sample treatment

The water samples were collected at the different sample sites (A1-A7/B1-B2), on several days over three weeks, starting on July 17 until August 8, 2018. On each of the seven sample days (July 17/19/22/29 and August 1/4/8 2018), one sample was collected at each sampling site, resulting in a total of 58 samples. The sample sites A4-A7 and B1 were not sampled on August 4. The volume of the collected stream water varies between the days and sample sites. By filtering the water with a 0.45-µm glass fibre filter it was determined that the contained C was DOC. For preservation, 1 µL of 3 mol/L HCl solution per 1 mL stream water sample was added which acidified the samples to a pH level of around 2. The samples were then stored at 3°C in the dark until further analysis in February 2021.

The year 2018, as the second warmest year on record (1979-2018) was characterized by a widespread of droughts in Northern Europe (Ramonet et al. 2020; European Arctic | Copernicus 2021 - assessed February 2021). The significantly warmer temperature and reduced soil moisture influenced the C-cycle in multiple ways (Ramonet et al. 2020). Thus, analysing the DOC dynamic during this year in a discontinuous permafrost was of great interest.

Studies show that there is no impact on the DOC caused by the preservation method used to store the samples (filtered, acidulated, dark, and refrigerated). Chen and

Wangersky (1996) demonstrated no detectable loss of DOC if samples are acidified with HCl and stored refrigerated (2°C) after 145 days. This method prevents bacterial degradation and physical loss for short and long periods. Moreover, Chen and Wangersky (1996) state that this preservation method of DOC is also applicable for DOC samples with high labile organic compounds. Likewise, Walker et al. (2017) showed that there is no systematic change in DOC concentration and DOC isotopic composition when samples are acidified (with 1 mL 85% H_3PO_4) before being stored. Barely any loss of DOC was noticed over the 380 days of storage in the study from Walker et al. (2017), furthermore, the small amount of DOC loss is not related to the storage time as such, rather attributed to acidification (Walker et al. 2017). Thus, although the storage in the current work was longer, there are good reasons to assume that the DOC was not affected by the storage.

2.5 Experimental design

For the DOC analysis, four experiments were performed. To understand the link between bioavailability and DOC traits, DOC concentration, stable C isotopic composition (^{12}C and ^{13}C), optical characterization (a250/a365), and biodegradation of the DOC were analyzed. The determination of the DOC concentration helped identify from which region within the Stordalen catchment the highest amount of DOC was derived. Stabil C isotope signature served to detect in which region the DOC is most degraded. For the optical characterization analyses, an Aqualog was used to explore the chemical composition of the DOC, whereby conclusions about the degradation of DOC could be made (Berggren et al. 2020). Furthermore, with this analysis, it was possible to determine whether the DOC is characterized by low-molecular weight and thus boilabile or by high-molecular weight and recalcitrant (John et al. 2008; Xenopoulos et al. 2021). The biodegradation experiment revealed the oxygen concentration over the incubation time and identified in which region of the Stordalen catchment an increased degradation occurs (Berggren et al. 2020). For the calculation of the daily DOC degradation, the DOC concentration values were used as well. Between the different experiments, the samples were returned to the storage condition (3°C and dark).

2.5.1 DOC concentration and stable carbon isotope signature

The DOC concentration of the samples, as well as the stable C isotope signature, were carried out externally. Protected from light exposure, the samples were shipped for analysis.

2.5.2 DOC optical characterization

The analysis of the optical characterization was done with the undiluted samples which were kept acidified. Four mL of each water sample was transferred into a 1 cm-quartz cuvette, which had been rinsed three times with purified water and once with sample

water before finally filling it with the sample water. The cuvette was washed with ethanol (ethanol absolute ≥99.5%) and rinsed with purified water (6 times) at the beginning of the experiment and again after having processed approximately 12 samples. To ensure that no deflection was caused on the walls of the cuvette, its outer walls were cleaned with ethanol each time before the cuvette was placed in the Aqualog.

For the settings of the Aqualog VS140 (Horiba Jobin Yvon, Edison, NJ USA), an extraction wavelength from 230 – 600 nm, with an increment of 5 nm was set. The emission wavelength was from 214.48 – 624.01 nm with an increment of 3.28 nm (8 pixels) and the CCD gain was medium. The integration time (exposure time) was 2 seconds. Before starting the experiment, the fluorescence excitation-emission spectra of an ultrapure water blank were measured for inner filter effects (Berggren and Giorgio 2015). The data was processed with the AQUA (Aqualog V3.6) program and further analyzed with Microsoft Excel (Version 2105).

2.5.3 DOC biodegradation

For the respiration monitoring experiment, which analyses the dark oxygen consumption over time, the samples had to be re-adjusted to their original levels. Therefore, the temperature, the pH, and the microbial community had to be restored. For the pH re-adjustment, a 1 mol/L NaOH solution was produced by dissolving 40.00 g of Natriumhydroxid pellets in 1 L of purified water. Then the samples rested until all pellets were dissolved (resting time 24h). For storage, the 1 mol/L NaOH solution was transferred into a 100 mL Duran bottle and stored in the dark at 3°C. To adjust the pH to the original level, 3 µL of the 1 mol/L NaOH was added to 1 mL of water sample as a fixed value. After 24 hours, the pH was checked by placing a drop of the sample on a pH indicator paper using a Pasteur pipette. Due to irregularities, the pH of each sample was checked and, if needed, adjusted to a level between pH 5-8. This was done by adding again NaOH or in a very few cases (two samples) HCl. Further adjustments to the samples were made shortly before the respiration monitoring started. Therefore, each sample was microbial inoculum with 2% of an inoculum to reach equal microbial starting conditions. The microbial inoculum was a mixture of different stream waters from regions in northern Sweden and became enriched (50:50) with fresh (sampled 15.03.2021) stream water from the Abisko region (Abiskojåkka), to become a diverse inoculum with different bacterial strains. To avoid contamination, the sensor vials were washed with ethanol (ethanol absolute ≥99.5%) and rinsed six times with purified water to remove any ethanol residue. Afterwards, the decay experiment was processed (Berggren et al. 2020). To do so, the pH and microbial adjusted samples were injected in the cleaned 5 mL sensor vials and airtight sealed with a butyl rubber septa cap. The sensor vials were maximally filled with sample water and closed without headspace or

air bubbles. The vials have a Sensor Dish Reader (SDR) at the bottom (PreSens Precision Sensing, Regensburg, Germany). For incubation, the SDR vials were placed on a 24-multiwell plate, and each well was placed on the SDR reader that was positioned in a climate chamber (ESPEC, Japan). The temperature in the climate chamber was set to 20°C. The air pressure in the climate chamber was 967 millibar. Every 2 h, over 14 days, the dissolved oxygen (DO) concentration (mg/L) was automatically measured by the SDR reader and processed by the PreSens (SDR_v4.0.0) program. To avoid instrumental uncertainty duplicates of each sample were performed.

2.6 Data analysis

2.6.1 DOC concentration and stable carbon isotope signature

DOC concentration and the composition of stable C isotope (given as $\delta^{13}C$) were provided in mg/L and per mille (‰) respectively. The $\delta^{13}C$ indicates how much the $^{13}C/^{12}C$ ratio of the analysed sample differs from the internationally accepted standard Pee Dee Belemnite (PDB) in per mille.

2.6.2 DOC optical characteristics

The spectroscopic parameter a250/a365 was defined by calculating the ratio between the spectrophotometric absorption of the 250 nm and 365 nm. For the sub-catchment A3 of sampling day 29 July, the values were marked as an outlier and not included in further calculation.

2.6.3 DOC biodegradation

After 14 days of incubation, the measurement was concluded and the data, which included DO [mg/L] in 2-h-intervals over the measurement time, were subjected to quality control with Microsoft Excel. Thereby, the DO concentration over the measurement time was plotted to identify possible outliers. Two samples (A5 from 29.7. and B1 from 19.7.) were marked as outliers as their curves dropped to a DO concentration of zero right at the beginning and therefore showed a strikingly different trend than the rest. Hence, only single values were used for further analysis of these samples, instead of duplicates as with the others. For samples with replicates, the mean was taken for analysis.

The plotting of the DO over time revealed that there was no decrease within the first 24 hours. The slope showed a plateau. In the context of bacterial growth, this is called a lag phase and characterized by low bacterial activity due to adaptation of the cells to the medium (Rolfe et al. 2012). To avoid this influence, the data from the first 24h of the experiment were not used in the analysis.

For the conversion of DO to bacterial respiration which corresponds to C biodegradation, the slope of DO concentration over the incubation time which was converted to days was calculated. Subsequently, the slope was multiplied by 12/32, which is the molecular mass ratio between C and O_2, respectively (Hensgens et al. 2020). Furthermore, it was multiplied by the respiration quotient (RQ). In this case, an RQ of 1 was assumed, as this is a common RQ that has been measured both in soil and for DOC degradation in aquatic systems (Berggren et al. 2012; Hensgens et al. 2020). The result represented the daily DOC degradation.

The calculation of the DOC concentration at any time step (DOC_t) was done by using Equation 1 (Hensgens et al. 2020). Therefore, the initial DOC concentration (t=0), the DO concentration at any time step ($O2_t$), the molecular weight of C (C_{mass}), and O_2 ($O2_{mass}$) were needed. Both concentrations were given in mg/L. Here as well, a RQ of 1 was assumed.

Equation 1:

$$[DOC_t] = \left(\frac{[DOC_{t=0}]}{C_{mass}} - \frac{[O2_{t=0}] - [O2_t]}{O2_{mass}}\right) C_{mass}$$

To detect how the DOC concentration at the different sample sites developed over the incubation experiment, the mean value of the DOC concentrations from the different sample days was calculated and plotted for each sample site. For the DOC concentration of the sub-catchment A7 some values dropped below zero. As DOC concentration cannot be negative, these values were removed for further analysis, as the sensors at the bottom of the vials seemed to be broken.

2.6.4 Statistical analysis

As the water samples were taken on different days over a period but were considered as replicates from a sub-catchment, autocorrelation occurred and was confirmed by the Durbin Watson test. To avoid significance between the tested variables due to autocorrelation, the significance level of $\alpha = 0.05$ was set to $\alpha = 0.01$ (Berggren et al. 2018). Though models such as the linear mixed-effects model could account for time autocorrelation, an α of 0.01 was taken, as it could also be used to test for correlation (Berggren et al. 2018). An α of 0.05 was used to test for normality.

The statistical analysis was performed with the computer program R (R version 4.0.2). For the correlation test (Kendall's rank correlation tau test), the package *psych* with the function *pairs.panels* was applied. Additionally, according to this function, for variables that were significantly correlated the p-value was calculated. The four continuous variables, DOC concentration, $\delta^{13}C$, a250/a365, and daily DOC degradation

were tested for correlation against sub-catchment elevation, slope, relief, area, and peatland cover. As the tested variables were not normally distributed (Shapiro-Wilk normality test: $p<0.05$), Kendall's rank correlation tau test served as the correlation method.

A multiple linear regression (*lm-function*) model was used to analyse which of the morphological variables (sub-catchment elevation, slope, relief, area, and peatland cover) significantly influence the DOC concentration, $\delta^{13}C$, a250/a365, or daily DOC degradation over the entire Stordalen catchment. Therefore, four multiple linear regression models were created, one for each DOC property (dependent variable): DOC concentration, $\delta^{13}C$, a250/a365, or daily DOC degradation. The morphological variables were set as predictor variables and with the stepwise selection method, the variables which significantly account for the DOC property were selected. This was done with the package *olsrr* and the function *ols_step_both_p*. The stepwise selection function entered and removed predictor variables in all possible combinations based on p-values until the best model fit was found with predictors that significantly contribute to the dependent variable. Before adding/removing the next predictor variable to the model, a comparison was done to assess whether the modified model was significantly better at predicting the outcome variable. This is called cross model comparison (Mzobe et al. 2018). The stepwise selection procedure was the same for all DOC property models.

The models were visually proved and if needed transformed (log10 transformation). All dependent variables had to be transformed. The visualization was done by creating a residual vs. fitted and a QQ-plot to test for normal distribution of the residuals and non-linearity, respectively.

To identify whether a difference in the lability classes between the different regions exists, on the basis of the morphological data and the peatland cover, the sub-catchments were divided into two groups. A1-A6 made up one group and A7 and B1/B2 formed the other. To test the differences a non-parametric unpaired t-test (Wilcoxon rank-sum test) was applied, as the data was not normally distributed (Shapiro-Wilk normality test: $p<0.05$). With the non-parametric unpaired t-test the final DOC concentrations, between the two groups and the loss of DOC over the time of the incubation were tested and compared.

3 Results

The obtained results of the different DOC properties (DOC concentration, stable C isotopic signature, a250/a365, daily DOC degradation) for each sub-catchment can be seen in Table 3. This serves as an overview, while in the following subsections the results of each DOC property, combined with the statistical analysis results are described in more detail.

Table 3. *Mean ± standard deviation of DOC concentration [mg/L], stable C isotopic signature ($\delta^{13}C$) [‰], DOC optical characteristics (a250/a365), and daily DOC degradation [mg/L] from the different sub-catchments (A1-A7 and B1/B2). A1-A3 and B1 n=7, A4-A7 and B2 n=6. For daily DOC degradation duplicates were measured, thus 2*n.*

Sub-catchment	DOC concentration [mg/L]	stable C isotopic signature ($\delta^{13}C$) [‰]	DOC optical characteristic a250/a365 [cm^{-1}/cm^{-1}]	Daily DOC degradation [µg C/ L/ d]
A1	1.84 ± 0.05	-28.76 ± 0.1	6.42 ± 0.30	26.47 ± 6.14
A2	2.13 ± 0.24	-28.72 ± 0.15	6.29 ± 0.29	33.94 ± 7.26
A3	1.94 ± 0.26	-28.54 ± 0.18	6.56 ± 0.35	31.96 ± 5.23
A4	2.50 ± 0.30	-28.24 ± 0.14	6.57 ± 0.50	27.38 ± 6.59
A5	2.92 ± 0.32	-28.53 ± 0.13	6.06 ± 0.13	31.89 ± 5.06
A6	2.77 ± 0.42	-28.77 ± 0.08	6.13 ± 0.56	72.76 ± 21.80
A7	1.24 ± 0.12	-28.78 ± 0.18	7.00 ± 0.36	91.08 ± 24.04
B1	3.80 ± 1.30	-28.20 ± 0.31	6.40 ± 0.55	80.25 ± 19.53
B2	2.97 ± 0.39	-27.97 ± 0.09	6.98 ± 0.23	74.50 ± 8.10

3.1 Statistical analysis

The stepwise selection of the multiple linear regression showed that $\delta^{13}C$, a250/a365, and daily DOC degradation could be predicted with a selection of the chosen morphological variables (Table 4). However, DOC concentration was not significantly predictable with any of these variables and was therefore not further considered in the context of this regression analysis. The multiple linear regression model revealed that the variable slope had a significant impact on $\delta^{13}C$ and a250/a365, accounting for 25% and 21% respectively of the variance. For the daily DOC degradation, it was peatland cover and relief, accounting for 59% (Table 4). Other morphological parameters did not show any significant influence, on $\delta^{13}C$, a250/a365, or on the daily DOC degradation.

***Table 4**. Multiple linear regression models for delta13 (lm_delta13), a250/a365 (lm_a250/a365), and daily DOC degradation (lm_decay). DOC property (dependent variable) ~ predicted variables. Morphological variables were set as predicted variables (peatland cover, relief, area, slope, and elevation) and with the stepwise selection, the significant predictor defined, if p-value < 0.01. For all variables n = 58 except a250/a365 n =57.*

Model name	Model	R^2 (adjusted)
lm_delta13	Model_delta13 = delta13 ~ slope	0.25
lm_a250/a365	Model_a250/a365 = a250/a365 ~ slope	0.21
lm_decay	Model_daily decay = daily decay ~ peatland cover + relief	0.59

The results from Kendall's rank correlation tau test (Table 5) supported the results of the linear regression i.e., the DOC concentration was not related to the tested morphological variables. All p-values were > 0.01 when DOC concentrations were tested for correlation with the morphological variables.

To bring the different DOC properties into context, these were plotted together with the elevation for each sub-catchment (Figures 3-6). Moreover, the different plots represent the DOC properties at the different sub-catchments. All morphological variables were significantly correlated with each other, with exception area (Appendix: Table AII). Elevation, relief, and slope were negatively correlated with peatland cover, while relief, slope, and area were positively correlated with elevation. As these correlations were not the focus of this work, data are presented in the appendix and the information was used but not further discussed.

Table 5. *Correlation matrix (bivariable correlation) as an output of Kendall's rank correlation tau test. Tested correlations between relief, slope, area, peatland cover of the sub-catchment with data obtained from this (DOC concentration = DOC conc., $\delta^{13}C$, daily DOC degradation = DOC decay, a250/a265). Morphometric data are from Mzobe et al. (2020) except peatland cover (Olefeldt et al. 2013). Values represent the tau correlation coefficient. An α = 0.01 was used. Significant codes p-value ≤ 0.0001 "***", p-value ≤ 0.001 "**", p-value ≤ 0.01 "*". For all variables n = 58 except a250/a365 n =57. Numbers represent the tau correlation coefficient.*

	elevation	**Relief**	**Slope**	**Area**	**Peatland cover**	**DOC conc.**	**$\delta^{13}C$**	**DOC decay**
Peatland cover	**-0.44 *****	**-0.49 *****	**- 0.60 *****	-0.15				
DOC conc.	0.21	0.04	0.08	0.14	0.02			
$\delta^{13}C$	**0.33 ***	0.18	**0.25 ***	0.16	-0.25	**0.41 *****		
DOC decay	**0.42 *****	**0.38 ****	**0.35 ****	0.17	**-0.45 *****	0.16	0.11	
a250/a365	**0.30 ***	**0.37 ***	**0.39 ****	0.20	**-0.38 *****	-0.10	0.20	**0.22 ***

Table 6. *Best model fit of the regression models (lm_delta13, lm_a250/a365, lm_decay). All model values are log10 transformed. Df = degrees of freedom, α = 0.01. Significant codes p-value ≤ 0.0001 "***", p-value ≤ 0.001 "**".*

DOC property (dependent variable in the LM_model)	**Morphological variable (predicted variable in the LM model)**	**Estimate**	**Std. Error**	**Df**	**p-value**
$\delta^{13}C$	slope	-0.018	0.004	52	< 0.0001 ***
	intercept	0.376	0.039	52	< 0.0001 ***
a250/a365	slope	0.006	0.002	55	< 0.001 **
	intercept	0.757	0.014	55	< 0.0001 ***
daily DOC degradation	peatland cover	-0.062	0.011	50	< 0.0001 ***
	relief	0.001	0.0002	50	0.002 **
	intercept	2.025	0.149	50	< 0.0001 ***

3.2 DOC concentration

The DOC concentration for all sub-catchments ranged from 1.24 ± 0.12 to 3.80 ± 1.3 mg C/L (Table 3 and Figure 3). The lowest DOC concentration was detected in sub-catchment A7, while the highest concentration was found in sub-catchment B1. As seen in Figure 3, no clear visible increase or decrease in the DOC concentration corresponded with a change in elevation of a sub-catchment. This was further confirmed by the lack of correlation between elevation and DOC concentration. Moreover, the DOC concentration did not show a correlation with any tested variables. This is in line with the results from the stepwise selection, which detected no significant influence from the tested morphological variables.

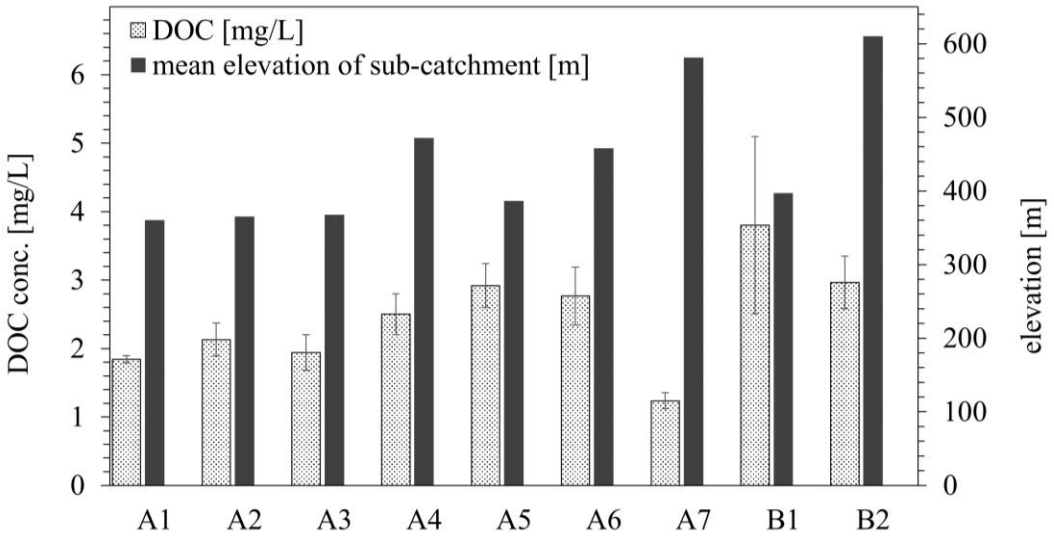

***Figure 3**. DOC concentration [mg/L] of different sub-catchments within the Stordalen catchment. The dotted bar charts represent the mean DOC concentration of all samples from this sample site, while the error bars represent the standard deviation of these samples (A1-A3 and B1 n=7, A4-A7, and B2 n=6). The black bars show the mean elevation of the corresponding sub-catchment. Elevation data from Mzobe et al. (2020).*

3.3 DOC stable carbon isotope signature

The range of the obtained values from the stable C isotope signature ($\delta^{13}C$) was very narrow, ranging from -27.97 ± 0.09 to -28.78 ± 0.18‰ (Table 3 and Figure 4). The most negative $\delta^{13}C$ was found in A7, while the least negative $\delta^{13}C$ was found in sub-catchment B2, followed by B1. Sub-catchment B2 with the least negative $\delta^{13}C$ showed the highest elevation (Figure 4). The positive correlation between $\delta^{13}C$ and mean elevation was confirmed by Kendall's rank correlation tau test (p-value <0.002, tau=0.33; Table 5). Furthermore, a moderately positive relationship was found between $\delta^{13}C$ and DOC concentration (p-value < 0.0001, tau = 0.41). With higher DOC

concentrations the $\delta^{13}C$ was less negative. The positive correlation between $\delta^{13}C$ and slope is on the threshold of being significant (p-value = 0.01, tau = 0.25). However, the regressions model indicated that $\delta^{13}C$ was significantly predicted by the slope (Table 6). This association was negative, meaning that an increase in slope corresponds with a more negative $\delta^{13}C$ value.

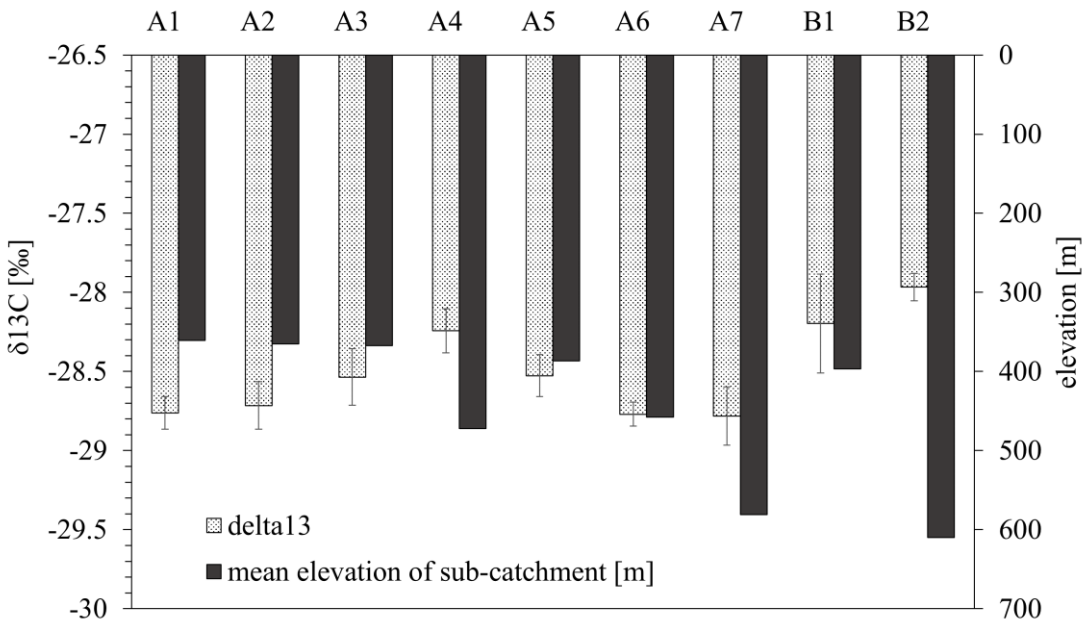

Figure 4. *δ13C [‰] values of different sub-catchments within the Stordalen catchment. The dotted bar charts represent the mean $\delta^{13}C$ of all samples from this sample site, while the error bars represent the standard deviation of these samples (A1-A3 and B1 n=7, A4-A7, and B2 n=6). The black bars show the mean elevation of the corresponding sub-catchment. Elevation data from Mzobe et al. (2020).*

3.4 DOC optical characterization

The a250/a365 values ranged from 6.06 ± 0.13 to 7.00 ± 0.36 (Table 3 and Figure 5**Error! Reference source not found.**). The highest a250/a365 was detected in sub-catchment A7, while sub-catchment A5 exhibited the lowest value. A7 was the sub-catchment with the second highest mean elevation. The relationship between elevation and a250/a365 was confirmed by Kendall's rank correlation tau test, showing a positive significant correlation between them (p-value = 0.002; tau = 0.30). Furthermore, a positive correlation between a250/a365 and relief, as well as slope existed (p-value < 0.001; tau = 0.37 and p-value < 0.0001; tau = 0.39 respectively). The lowest a250/a365 were found in the sub-catchment A5, which had the highest peatland cover fraction. Thus, with an increase in peatland cover, the a250/a365 values decreased. This was further supported by the negative correlation, represented by the results of Kendall's

rank correlation tau test (p-value < 0.001; tau = -0.38). According to the results of the regression analysis, the a250/a365 was significantly predicted by the slope (Table 6). As the relationship was positive, an increase in slope corresponds with a higher a250/a365 value.

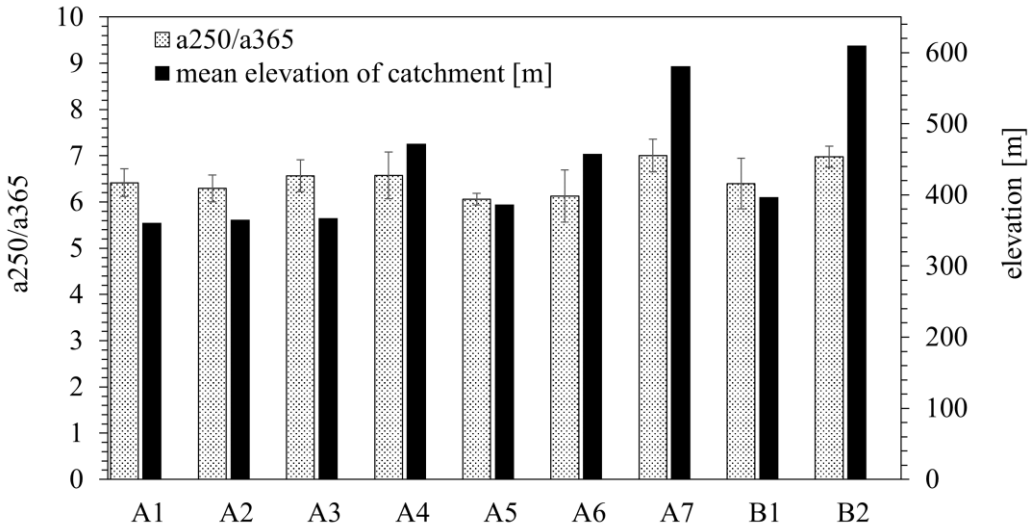

Figure 5. *a250/a365 values of different sub-catchments within the Stordalen catchment. The dotted bar charts represent the mean a250/a365 of all samples from this sample site, while the error bars represent the standard deviation of these samples (A1-A3 n=7, A4-A7, and B1/B2 n=6). The black bars show the mean elevation of the corresponding sub-catchment. Elevation data from Mzobe et al. (2020).*

3.5 DOC biodegradation

The daily DOC degradation over the incubation time ranged from 26.47 ± 6.14 to 91.08 ± 24.04 µg C/L/d (Table 3), with a clear separation between sub-catchments A1-A5 < 33.94 ± 7.26 µg C/L/d and A6, A7, B1, and B2 > 72.76 ± 21.80 C/L/d. Thus, sub-catchments A1-A5 all represented a similar daily DOC degradation rate and were all (except A4) among the sub-catchments with the lowest mean elevation (Figure 6). The Kendall's rank correlation tau test revealed a significant positive relationship between mean elevation and daily DOC degradation (p-value < 0.0001; tau = 0.42; Table 5). The correlation was reversed between daily DOC degradation and peatland (p-value < 0.0001, tau = -0.45). Both showed a moderate correlation to daily DOC degradation, presented by the tau correlation coefficient. Furthermore, a significant positive correlation was detected between daily DOC degradation and both relief and slope (both p-value < 0.001; Table 5).

The lm_decay model detected that both peatland and relief had a significant regulation on the daily DOC degradation and together, they predicted 59% of the DOC degradation (Table 4). Other morphological variables did not significantly regulate the daily DOC degradation rate.

Peatland cover had a negative relationship on the daily DOC degradation with a change of -0.06 ± 0.01 µg C/L/d for every unit increase in peatland cover (Table 6). This trend is further visualized in Figure 7. With an increase in peatland cover, the daily DOC degradation decreased. Sub-catchments with a lower peatland cover (A7, B1, and B2) showed a higher daily DOC degradation, with the exception of A6, which had a higher peatland cover and a higher degradation. This dependency between peatland and daily DOC degradation was detected by both Kendall`s rank correlation tau test and the regression model. Opposite to the peatland cover, the relief had a positive correlation on the daily DOC degradation rate. With an increase in relief, the degradation rate increased as well (0.001 ± 0.0002 µg C/L/d; Table 6).

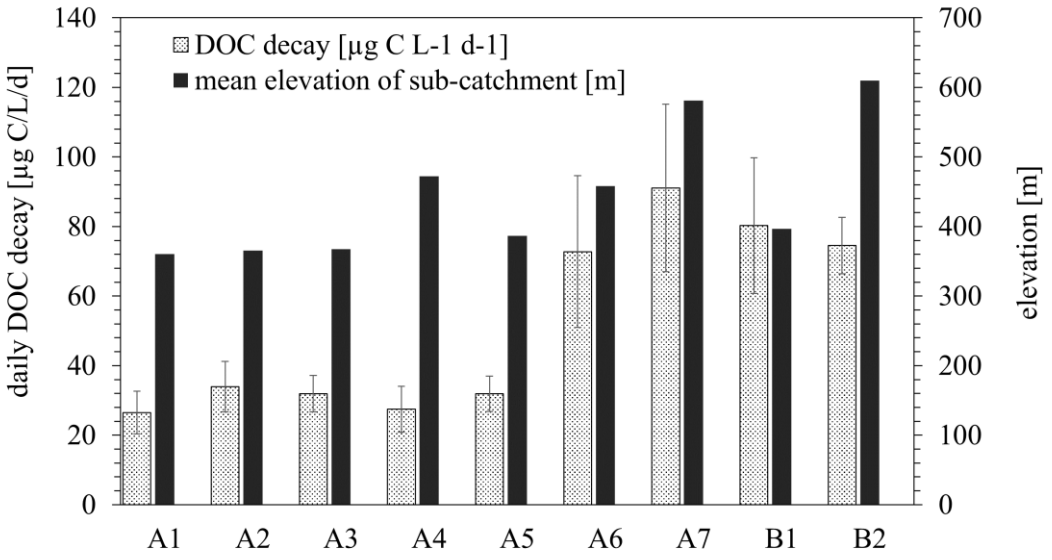

Figure 6. *Daily DOC loss [µg C/L/d] values of different sub-catchments within the Stordalen catchment. The dotted bar charts represent the mean daily DOC degradation of all samples from this sample site, while the error bars represent the standard deviation of these samples (duplicates were measured: A1-A3 and B1 n=2*7, A4-A7 and B2 n=2*6). The black bars show the mean elevation of the corresponding sub-catchment. Elevation data from Mzobe et al. (2020).*

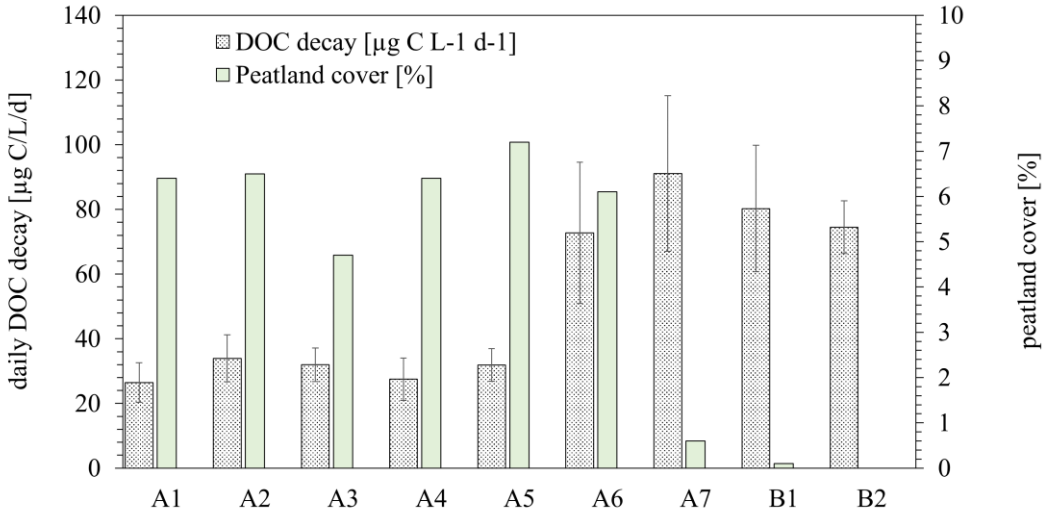

Figure 7. *Daily DOC loss [µg C/L/d] of different sub-catchments within the Stordalen catchment. Green bar charts represent the mean daily DOC degradation of all samples from this sample site, while the error bars represent the standard deviation of these samples (duplicates were measured: A1-A3 and B1 n=2*7, A4-A7 and B2 n=2*6). The grey bars show how much of each sub-catchment (%) is covered by peatland and the data are from (Olefeldt et al. 2013).*

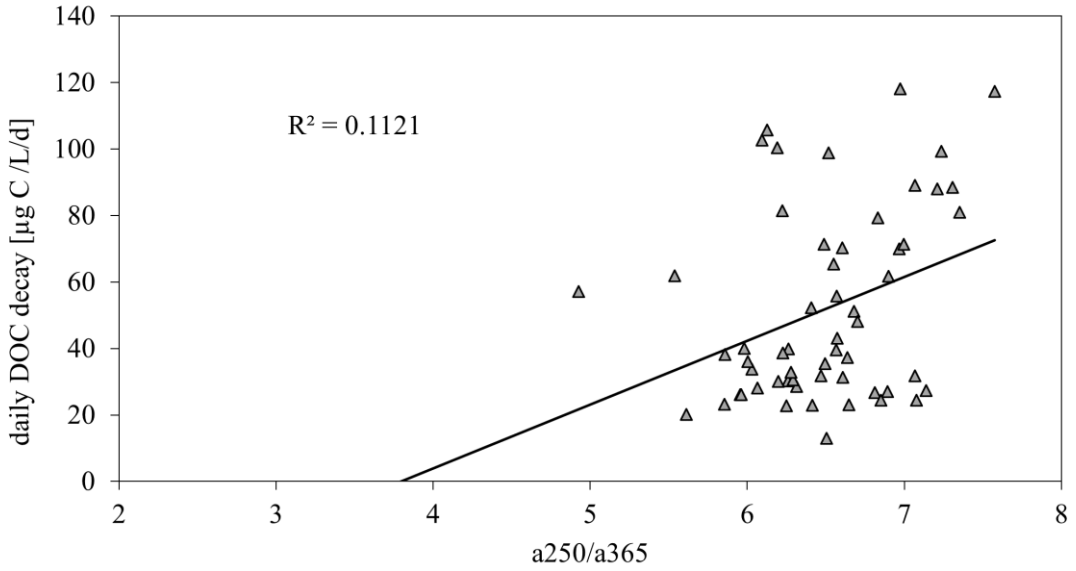

Figure 8. *Positive correlation between daily DOC decay and a250/a365. With an increase in the a250/a365 values the daily DOC degradation rate increased as well. The black line represents a linear trendline. n = 57.*

The association between the a250/a365 values with the daily DOC decay rate showed that there was a positive correlation (Table 5 and Figure 8**Error! Reference source not found.**). The Kendall's rank correlation tau test presented a weak, on the edge of being significant, positive correlation (p-value = 0.01; tau = 0.22; n = 57). This indicates that with an increase in the a250/a365 values the daily DOC decay increased as well.

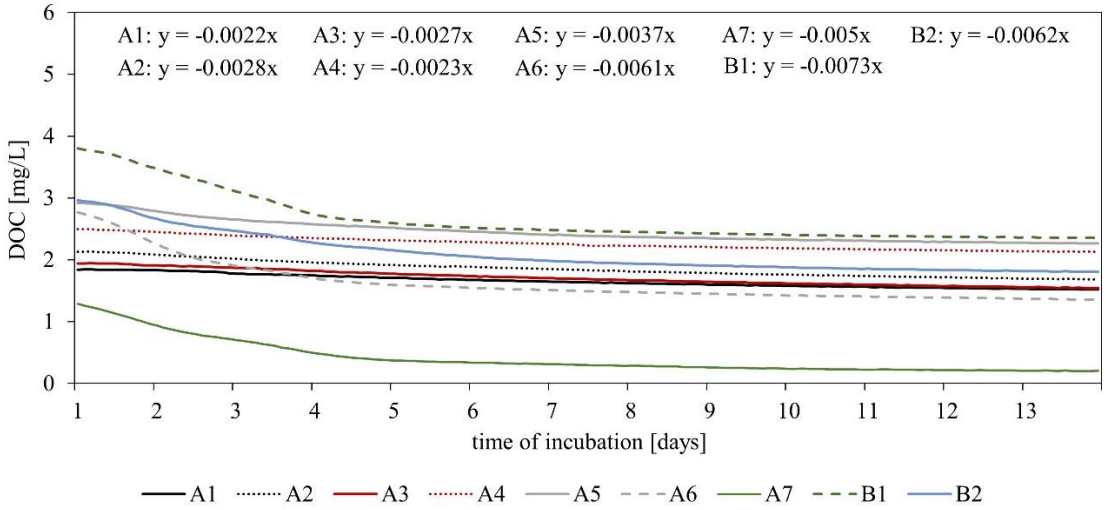

Figure 9. *DOC concentrations [mg/L] over the incubation time at all sample sites (A1-A7/B1-B2). Incubation time was 14 days, however, the first 24h were removed. Line graphs represent the mean of all sample sites and duplicates, which are additionally presented in Table 7 (A1-A3 and B1 n=2*7, A4-A7 and B2 n=2*6). Equations present the linear trendline equation without the intercept of each sub-catchment.*

Figure 9 supports findings that have already been presented in the previous section. Sub-catchments A7 and B1/B2 showed a higher DOC degradation than the other sub-catchments, identified by steeper slopes (displayed in Figure 9) and thus an increased loss of DOC. The visual analysis of Figure 9 showed that within the first 5 days of the incubation experiment, the DOC degradation rate was strongest, followed by only minor DOC level decreases from thereon. This is especially true for the sub-catchments A7 and B1/B2 as well for sub-catchment A6. Contrarily, A1-A5 showed DOC degradation rates that were rather constant over the entire incubation time. The trendline of the sub-catchments A1-A4 showed the flattest slope, A5 displayed an intermediate slope, while A6/A7 and B1/B2 had the steepest slope.

This is further presented in Table 7, as the loss of DOC (difference between initial and final DOC concentration) is higher for the sub-catchments A6/A7 and B1/B2. The results from the non-parametric unpaired t-test detected a significant difference in the loss of DOC between the two groups (A1-A6 vs. A7 and B1/B2) (Wilcoxon rank-sum

test: $p < 0.0001$, for A1-A6 n = 39, for A7 and B1/B2 n = 19). However, the final DOC concentration did not differ significantly between these groups (Wilcoxon rank-sum test: $p = 0.55$).

Table 7. *Mean DOC concentrations [mg/L], initial concentration, after 14-days incubation, and the differences between these from the sub-catchments (A1-A7 and B1-B2) from the Stordalen catchment. The table shows the mean of all sample sites and duplicates, which are visualise in Figure 9 (A1-A3 and B1 n=2*7, A4-A7 and B2 n=2*6).*

	A1	**A2**	**A3**	**A4**	**A5**	**A6**	**A7**	**B1**	**B1**
Initial DOC concentration [mg/L]	1.84	2.13	1.94	2.50	2.92	2.77	1.29	3.8	2.97
Final DOC concentration after incubation [mg/L]	1.52	1.68	1.54	2.12	2.26	1.35	0.20	2.35	1.80
Difference in DOC concentration [mg/L]	0.32	0.45	0.40	0.38	0.66	1.42	1.09	1.45	1.17

4 Discussion

Even though the results may not show a relationship between all morphological variables and DOC properties, there might exist one indirectly as the morphological variables are correlated with each other (Appendix: Table AII). In sub-catchments located in higher areas less peatland cover occurs.

4.1 DOC concentration

All DOC concentrations found in the Stordalen catchments are lower than those measured in previous studies. Mzobe et al. (2020) for example, discovered a monthly mean DOC concentration of 10.6 ± 3.7 mg/L, with the lowest DOC concentrations in steep sub-catchments (e.g. B2 6.5 ± 3.1 mg DOC/L) and the highest in peaty lowland (e.g. A6 13.7 ± 2.6 mg DOC/ L) in the Stordalen catchment from 2007 to 2011. This is almost opposite to the results from this work. Additionally, the lowest DOC concentration found in the study by Mzobe et al. (2020) is considerably higher than the highest DOC concentration in this work.

The results from this work did not show *(i)* a higher DOC concentration from peat-influenced streams than from uplands, thus, the first hypothesis is rejected. The DOC concentration results from this work and the ones from Mzobe et al. (2018 and 2020) differ regarding their correlations with elevation, relief, slope, area, and peatland. In the study from Mzobe et al. (2018 and 2020), all variables except peatland were negatively correlated with the DOC concentrations and positively correlated with peatland cover. These trends were not found in this work. Furthermore, in this work, B2, the highest located sub-catchment, had one of the three highest DOC concentrations and B1, which is mainly located in mountainous regions and characterized by the steepest slope in the Stordalen catchment, was also a sub-catchment with one of the highest DOC concentrations. Thus, a higher mean elevation of a sub-catchment was not associated with lower DOC concentration or vice versa.

As peatland is more present in lowland areas, DOC concentrations from sub-catchments (e.g. A1-A3) in this work were expected to have a higher DOC concentration than sub-catchments in upland areas (e.g. B1). However, this was not the case. This is a very atypical phenomenon as many other studies have detected higher DOC concentrations in peatlands (Fellman et al. 2008; Olefeldt et al. 2013; Lambert et al. 2014; Mzobe et al. 2018 and 2020; Sebestyen et al. 2021).

Olefeldt et al. (2013) used the same sub-catchments in the Stordalen catchment as Mzobe et al. (2018 and 2020) and the current work. They found lower DOC concentrations in higher sub-catchment for the year of measurement 2007-2009.

Therefore, it can be assumed that the difference in DOC concentrations in this work might be related to the time of sampling. Water samples for the study from Olefeldt et al. (2013) were taken in autumn (2007 Sep. and 2008/09 Oct.) and Mzobe et al. (2020) combined the data from Olefeldt et al. (2013) with samples taken biweekly from May to mid-October. Sampling for this work took place in the summer of 2018 (July and August). The year 2018 was characterised by slightly lower annual precipitation and higher air temperature, resulting in higher evapotranspiration rates (see section 2.3). These dry conditions can lead to lower runoff or even stagnation and a lowering of the water table (Quinton and Marsh 1999; Carey 2003). Lower runoff results from an increased water storage, when the active layer re-thaws and deepens again towards summer (Quinton and Marsh 1999; Olefeldt et al. 2013). Thus, lower runoff in the time of sampling can result in lower discharge from the surrounding peat into streams, and therefore no input of DOC from the peaty lowland. The stream water during these times is then mainly originated from upstream.

The precipitation pattern does not differ markedly between the years of sampling from the aforementioned studies and this work. The cumulative mean annual precipitation for 2007-2011 was 298.6 ± 57.5 mm/year, which is in the range of the annual precipitation of 2018 (287.0 mm/year – detailed climate analysis in section 2.3). Also, the cumulative monthly precipitation pattern during the month of sampling did not differ a lot (2007-2011 80.7 ± 19.9 mm and 2018 94.1 mm). However, air temperatures did differ between these years for the sampling month. The daily mean air temperature for the years 2007-2011 was 10.6 ± 3.26°C (July and August) while for the year 2018, it was 12.6 ± 4.1°C (July and August). Combined with the precipitation data, it is evident that evapotranspiration was increased during 2018 (Peters et al. 2020), resulting in drier conditions in the region. Thus, it can be assumed that meteorological conditions influence the DOC export. The temperature was measured at the Abisko Scientific Research Station (Abisko Scientific Research Station, 2021; Meteorological data from Abisko Observation, daily mean 1985-01-01 – 2020-12-31), while the precipitation data were provided by SMHI.

A reverse hydrological case to the one explained above, which could also lead to a lower DOC concentration, can occur during stormflow events. DOC concentrations discharged from peatland are low during such events, as the peatland runoff is additionally diluted by perennial runoff from upland areas (Köhler et al. 2008; Sebestyen et al. 2021). The precipitation data showed that the cumulative amount of precipitation for July was below average, but if looking at the daily amount of precipitation, this was due to low precipitation in early July. The precipitation pattern was followed by days with rainfall above the average of the surrounding years.

However, at the beginning of August, less precipitation than average has been recorded. Thus, the runoff may have been diluted at the beginning of the sampling. Such an event can explain the higher DOC concentrations from upland areas, as it results in little evapotranspiration and a rising water table. A rising water table causes water to infiltrate into the upper organic layers. The OM that has accumulated there would then be solubilised and discharged (Fellman et al. 2008; Köhler et al. 2008). Furthermore, during increased runoff due to stormflow or after snowmelt events, the soil can be depleted due to flushing of soluble OC, which can subsequently lead to a lower DOC leaching (Carey 2003). This could be an explanation for the lower DOC concentration in this work.

The above-described events demonstrate that discharge in a catchment has a critical influence on the DOC concentration. Therefore, the total amount of released DOC is influenced by the DOC concentration and the discharge. Thus, the efflux of DOC is not only determined by the DOC concentration but also by the hydrological condition of the catchment area that controls the discharge. The hydrological condition depends next to catchment properties like soil, vegetation cover, topography also on soil moisture, rainfall amount and intensity before and during sampling (Haga et al. 2005). Unfortunately, the discharge was not measured during sampling and could not be acquired retrospectively. Therefore, a comparison of the DOC concentration between the current work and previous studies is difficult, as different discharges cause variability of the DOC concentrations.

However, as mentioned before, the evapotranspiration differed between this work and the aforementioned studies, resulting in different hydrological conditions and thus different discharges. This could cause the differences in the DOC concentrations between the previous studies and the current work, as well as the differences in the found correlations. Furthermore, the results were analysed based on an individual consideration of the sub-catchments and thus under the assumption that each sub-catchment represents a single unite and does not include upstream values. Due to this, the origin of the DOC from a single catchment is unknown. It could either have originated from upstream sub-catchments and been transported downstream or derived from the surrounding sub-catchment. However, in this work, it is assumed that the surrounding sub-catchment has the strongest influence on the DOC properties.

Precipitation also influences the contribution of groundwater to the discharge (Olefeldt et al. 2013). According to Olefeldt et al. (2013), in wetter years more groundwater contributes to the discharge into streams than in drier years. The DOC concentration is lower in groundwater due to absorption of C in the mineral soils, resulting in lower DOC concentration in sub-catchments that receive groundwater (Carey 2003).

However, this is not an explanation for the pattern occurring in this work, as the sub-catchments receiving groundwater are B1 and B2 (Olefeldt et al. 2013), which comparatively did not have lower DOC concentrations. Furthermore, the DOC concentration of groundwater in the Stordalen catchment is around 5 mg C/L (Olefeldt and Roulet 2014), which is still above the concentrations obtained in this work.

Another reason for the differences can be that in upland regions the DOC was degraded before being transported downstream and therefore did not contribute to the DOC concentration in the lowlands (Striegl et al. 2005). Also, the presence of lakes can influence the DOC concentration at the different sub-catchments, as lakes serve as a DOC sink (Tranvik et al. 2009). In the Stordalen catchment, peatlands and lakes are spatially close to each other, occurring at a similar elevation and have a higher dominance in the lowlands (Mzobe et al. 2018). Therefore, a reason for the lower DOC concentration in peaty lowlands can be the presence of lakes.

Furthermore, another study carried out in 2018 in north Sweden and on the border to Norway, by Al-Kharusi (2021), showed that the DOM values were comparatively lower in this year compared to other, wetter years. As mentioned before, 2018 was characterized as a dryer year with increased evapotranspiration. According to Al-Kharusi (2021), unusually dryer periods have a negative influence on the DOM export. As the sampling for this work took place in 2018 as well this could be another influencing factor.

In general, the measured DOC concentrations in this study were markedly lower than in the above-mentioned studies. It can be speculated that the storage time caused the low DOC concentration values in this study. The time between sampling and analysis was nearly 3 years. Both studies, Chen and Wangersky (1996) and Walker et al. (2017), cited in the section Sample treatment (section 2.4) detected no significant loss of DOC in their preservation experiment, however, both did not exceed a storage time of 380 days which was the case in this work. Peacock et al. (2015) though found a strong relation between DOC loss and storage time which was about 20% DOC loss over 3 years. However, it is important to mention that the tested samples by Peacock et al. (2015) were compared to those in this study not acidified. A DOC loss of 11% over 2 weeks was proved by Kaplan (1994) when the samples were treated with acids. Furthermore, Wilson et al. (2020) found in their study a DOC deviation of the samples treated with HCl, filtered and stored at 4° C, especially in the $\delta^{13}C$ values. Deviation over time can be caused by DOC consumption by biological and microbial activity (Wilson et al. 2020). Thus, an appropriate preservation method and, if possible, short storage time is recommended (Kaplan 1994; Wilson et al. 2020). However, adding acid

to water samples can cause hydrolysis and thus a loss of OC and/or an alteration of DOC molecular composition (Kaplan 1994; Walker et al. 2017).

4.2 DOC stable carbon isotope signature

The received $\delta^{13}C$ values do not differ a lot between each other. When comparing them with previous studies, the stable C isotope signatures for all sub-catchments obtained here were in the range of the value more likely found in oxygen-limited peaty lowlands (Schaub and Alewell 2009; Lambert et al. 2014). Studies, carried out at a different study site, measured a $\delta^{13}C$ of -29.4‰ (Lambert et al. 2014) or -28.6‰ (Schaub and Alewell 2009) in wetlands, while for uplands with aerobic metabolism the $\delta^{13}C$ was -26.4‰ (Lambert et al. 2014) and -26.6‰ (Schaub and Alewell 2009). Therefore, it seems that the DOC in all sub-catchments from this work were characterized as isotopically lighter and thus contained more ^{12}C (Schaub and Alewell 2009). However, this would mean that in all sub-catchments a reduced degradation occurred, as decomposer preferable utilizes the isotopically lighter ^{12}C (Mu et al. 2014), even in well-drained upland areas.

Again, the storage of the samples may have influenced the results. As Wilson et al. (2020) found in their study, there was a slight decrease in $\delta^{13}C$ over 66 days. This may explain why the obtained $\delta^{13}C$ values in this study were all in the range of peatlands. Hence, it can be speculated that the C isotope signatures of the samples were altered by the storage as well and originally showed some values that were more in the range of uplands C isotope signature.

Nevertheless, a positive relation between elevation and $\delta^{13}C$ was detectable. Both sub-catchment B1 and B2, with the least negative $\delta^{13}C$, are located in well-drained upland areas, which allows higher degradation rates than water-saturated peatlands and thus an increased consumption of ^{12}C (Mu et al. 2014). Furthermore, clay minerals, which are more frequent in these sub-catchments, absorb ^{13}C-enriched components, resulting in DOC originates from these areas in a less negative $\delta^{13}C$ (Wynn et al. 2005).

However, no relationship with peatland cover, where less degradation occurs, was found. This might be caused by no uniform distribution of $\delta^{13}C$ between the different sub-catchments and only very slight differences. This was especially recognizable in sub-catchment A7 versus B2, both containing less than 1% peatland cover, but A7 showed the most negative $\delta^{13}C$, while B2 the least negative $\delta^{13}C$. Thus, other variables such as the slope also influenced the $\delta^{13}C$. With an increase in slope, the $\delta^{13}C$ values decreased. In sub-catchments with a steeper slope, more flushing and thus less accumulation of OM occurs (Hobbie et al. 2000). Thus, the negative estimation of $\delta^{13}C$ with increasing slope is open for discussion.

The positive correlation between $\delta^{13}C$ and DOC concentration is due to higher DOC concentrations in higher elevated sub-catchments, and as elevation is positively correlated with $\delta^{13}C$, the relationship between $\delta^{13}C$ and DOC concentration can be explained.

Concluding, according to the results, an enhanced degradation in DOC derived from the upland areas cannot be seen for the entire Stordalen catchment, only a few sub-catchments represented this.

4.3 DOC optical characterization

The obtained a250/a365 values in this work were higher than those from other studies. For example, Jiménez et al. (2014) detected in pore water of a peatland values ranging from 4.5 to 5.5. Also, in the study from Peuravuori and Pihlaja (1997), the obtained a250/a365 values of lake water were in a similar range. Comparing the a250/a365 values from this work with values from Olefeldt et al. (2013), a similar trend but also higher values were recognizable. Olefeldt et al. (2013) found the highest a250/a365 value in sub-catchment B2, around 5.2, while the lowest was found in sub-catchment A5 with 4.65. The high values from this work detected that the discharged DOC in all sub-catchment had a low aromaticity and were characterized as lower molecular weight DOC (Peuravuori and Pihlaja 1997; Su et al. 2015).

The differences between the values from Olefeldt et al. (2013) and this work could be caused by an increase of the active layer thickness at the study site. As discussed above, the temperatures differed during the time of sampling, with warmer daily air temperatures in 2018 than during the sampling of Olefeldt et al. (2013). Therefore, it can be assumed that permafrost degradation happened. At the study sites Storflaket and Heliport, both located in the region around Abisko, an increase in the thickness of the active layer occurred between the study period of Olefeldt et al. (2013) and 2018 (Strand et al. 2020). Thus, it can also be expected that the active layer deepened at the Stordalen mire and released lower molecular weight DOC. According to Drake et al. (2015), the deepening of the active layer releases freshly thawed OC, which is characterised by low-molecular weight. The release of low-molecular weight DOC could cause the higher values of a250/a365 in peaty lowlands, as these are the regions where permafrost occurs. However, this does not explain the higher values in upland regions compare to the previous studies.

Another possible reason for the higher values could be the preservation of the samples, as adding of an acid can lead to hydrolysis and thus a change in the quality of DOC (Kaplan 1994).

Regarding the obtained $\delta^{13}C$ values, the discharged DOC was determined as isotopically light. Thus, it was not detectable if the C isotopic signature changed with increasing active layer thickness. With increased deep in the soil profile C was exposed to enhanced degradation and thus an enrichment of ^{13}C (Mu et al. 2014). More measurements of optical characteristics and isotopic composition of DOC over several years in combination with the active layer thickness are needed. Additionally, it is important to know whether the runoff into the streams is determined by subsurface or overland runoff, as this influences the DOC (Quinton and Marsh 1999). The DOC source can either be from higher layers of the soil profile, characterized by high-weight molecules with an aromatic structure entering the streams with overland and near-surface flow, or from greater soil depth with low-molecular weight and subsurface flow (Xenopoulos et al. 2021).

High-molecular weight DOC was expected to be derived primarily from peatland areas as a reduced degradation of OM occurs due to water-saturation and thus anaerobic conditions (Schlesinger and Bernhardt 2013), but the a250/a365 values represented values associated with lower molecular weight for all sub-catchments. However, the statistical analysis detected that with an increase in the peatland cover the molecular structure of the released DOC was more complex. Thus, the derived DOC was less degraded when it originated from sub-catchments with a higher peatland cover fraction. Therefore, it can be answered that *(ii)* peatland-derived DOC is less bioreactive compared to upland derived DOC, but it must be considered that in general the divided DOC in this work was characterized by lower molecular weight.

The higher a250/a365 in sub-catchment A7 and B2, for example, could be caused by morphological variables. Both are located in mountainous regions and belong to the sub-catchments with the lowest peatland cover and the highest slopes, and thus, have a progressed C decomposition. As Hobbie et al. (2000) mention, topographical factors determine the accumulation of C and drainage, as these factors either promote peat formation in lower laying poorly drained wet areas or lead to flushing and downward movement on steeper slopes. A higher slope and relief lead to flushing of DOC instead of accumulation, the organic layer remains shallow in these areas and oxygen can diffuse into it and promote degradation (Fellman et al. 2008; Lambert et al. 2014). Therefore, DOC from upland areas was already more degraded than DOC derived from peaty lowlands, which was represented by a higher a250/a365 (e.g. A7 and B2). DOC originated from upland areas was, therefore, more bioreactive compared to DOC from peat-influenced streams, presented by a higher a250/a365. The influence of the morphological parameters was confirmed by statistical tests.

Furthermore, higher a250/a365 values could be influenced by groundwater. Sub-catchments B1 and B2 receive groundwater, according to Olefeldt et al. (2013). Mineral groundwater is characterized by low aromaticity with a more protein-like composition and therefore result in a higher a250/a365 (Olefeldt and Roulet 2014; Xenopoulos et al. 2021).

4.4 DOC biodegradation

The daily DOC degradation values from this work showed that a difference existed in the daily DOC degradation between DOC derived from upland areas and peaty lowlands. Sub-catchments A1-A5 (except A4), which are all located in lowland areas, are characterised by a low slope and relief and contain comparable higher peatland cover. These sub-catchments represented lower DOC degradation rates than sub-catchments determined by a higher mean elevation and lower peatland cover (e.g. A7, B1, and B2). This is supported by the correlation which detects a positive relationship between elevation, relief, slope, and daily DOC degradation, and a negative for peatland cover and degradation rate.

A6 represented a higher daily DOC degradation compared to A1-A5 despite a similar peatland cover. Thus, not only peatland cover is correlated to the degradation rate, but also other morphological variables. The results from the regression showed that additionally, relief had a significant influence on the daily DOC degradation. Thus, with a higher relief (e.g. A7 and B2) enhanced degradation occurred. However, the regression model further detected that peatland cover had a stronger influence on the DOC degradation rate compared to relief. In peatland, the degradation is reduced due to the lack of oxygen, and therefore, molecules with a comparable more complex structure were present, which are less degradable (Schlesinger and Bernhardt 2013; Xenopoulos et al. 2021). This was reflected by lower a250/a365 values and therefore lower degradation rate from sub-catchments in peatlands. However, the degradation rate of DOC has to be seen in the context of generally high a250/a365 values.

Both sub-catchment A6 and B1 showed a comparable lower a250/a365 and an enhanced daily DOC degradation. This contradicted the expectations but may be linked to the ratio of C and available nutrients, such as nitrogen or phosphorus as this also influences the DOC biodegradation (Coulson and Butterfield 1978; Mao et al. 2017). Thus, further research should include the nutrient availability at the different sub-catchments and the bacterial productivity.

However, this showed that degradation also depended on other influencing factors and explains why only 59% (R^2 of the linear regression model) of the DOC degradation could be explained with the selected morphological variables. Other predicted variables

that may also influence the DOC degradation and could therefore be, next to nutrients, lake cover, vegetation cover, water discharge, or proportion of upslope area contribution into sub-catchments. The inclusion of these variables may improve the prediction for the DOC concentration, $\delta^{13}C$ values, and a250/a365 and further, help to explain the patterns of the DOC concentration. Moreover, this is a possible explanation of why the correlation between a250/a365 and daily DOC degradation was weak. Nevertheless, this relationship revealed that DOC derived from upland regions has a higher decomposition rate than the DOC derived from peaty lowland regions, caused by a less complex molecular structure and an enhanced degradation of the C due to the presence of oxygen (Schlesinger and Bernhardt 2013; Xenopoulos et al. 2021).

The DOC concentration curves over the incubation experiment showed how much DOC was consumed by microorganisms over the time of the experiment (Figure 9). Microorganisms favour labile DOC, which is characterised by low-molecular weight C, as the cost-benefit is good (Fuchs et al. 2011; Beaupré 2015; Xenopoulos et al. 2021). Once it is exhausted, the semi-labile DOC will be utilised while the stable DOC remains (Hobbie et al. 2000; Drake et al. 2015; Xenopoulos et al. 2021). Thus, it was expected that DOC exported from upland areas have a higher biolabile share than from peaty lowland areas. This pattern could be seen in the DOC concentration curves. Especially the DOC concentration curve for the sub-catchments A6/A7 and B1/B2 have a steeper slope at the beginning of the incubation and level off with time. This suggests that the labile C was used as an energy source by microorganisms at the beginning of the incubation and with time as it became depleted the DOC concentration decreased slower as the semi-labile C is less easily degradable for microorganisms (Drake et al. 2015; Xenopoulos et al. 2021). A steeper slope of the DOC concentration curve, especially at the beginning, was mainly associated with the sub-catchments that contain less peatland cover and are higher elevated. Hence, DOC exported from these sub-catchments was further degraded, represented by a higher a250/a360 (e.g. A7 and B1) and thus more biolabile. Furthermore, the $\delta^{13}C$ values of sub-catchment B1 and B2 indicated that DOC from these areas had been exposed to increased decomposition. Moreover, the steeper slope of the DOC concentrations, for both sub-catchments B1 and B2 can additionally be caused by the groundwater contribution, as it contains more biolabile DOC (Olefeldt et al. 2013; Xenopoulos et al. 2021). The gentle slopes of the DOC concentrations of the sub-catchments A1-A4 showed that, in general, a lower DOC degradation was present here. Also, the lack of a steeper slope at the beginning indicates that the DOC derived from these sub-catchments contained less labile DOC, which could become rapidly consumed. This difference in the degradation of DOC is confirmed by the t-test, which presented a significant difference in the amount of DOC loss between the two groups of sub-catchments (A1-A6 vs. A7 and B1/B2). Therefore,

it can be concluded that *(iii)* DOC derived from peaty lowland was considered as semi-labile to recalcitrant DOC and the share of labile DOC was lower, compared to the DOC derived from upland areas. However, more intense analysis of the share of recalcitrant DOC derived from upland and peaty lowlands is needed as no significant difference in the DOC concentration at the end of the incubation was recognized. Furthermore, the final DOC concentration depends on the initial DOC concentration. In general, the results revealed that the proportion of recalcitrant or semi-labile degradable DOC was similar for uplands and lowlands after the incubation time. To distinguish between semi-labile and recalcitrant DOC, the incubation time of the experiment should be extended.

The dominant vegetation of a sub-catchment determines the composition of the litter and thus its degradation potential. Litter from deciduous species decomposes faster than litter from mosses (Hobbie et al. 2000). Thus, in areas where birch trees grow, higher elevated sub-catchments (e.g. A6, A7, B1, and B2) a higher decomposition rate existed. Furthermore, mosses are mainly dominant in peaty lowlands, and in addition *Sphagnum* spp. is low in nutrient concentration, which plays, as already mentioned, a determining role in degradation processes (Coulson and Butterfield 1978; Mao et al. 2017). Moreover, the released C from *Sphagnum* spp. vegetated peatlands consists of recalcitrant compounds (Hodgkins et al. 2016). Hodgkins et al. (2016) found less degraded and thus more aromatic compounds in *Sphagnum* spp. dominated area. This could also be seen in the results of this work, as in areas where *Sphagnum* spp. is present, which is limited to peatlands, the degradation rate was lower.

5 Conclusion

Analysed water samples from the discontinuous permafrost at the Stordalen catchment for the year 2018 showed *(i)* no higher DOC concentration in peat-influenced streams. There is no consistent trend indicating that higher concentrations occurred rather in one area than in the other, but there was a slight tendency towards higher DOC concentrations from upland sub-catchments. The DOC concentrations generally showed low values compared to other studies. However, due to the lack of discharge measurements for this study, a comparison with other studies is difficult, as discharge has a strong influence on the DOC concentration.

Regarding the molecular weight, differences between uplands and lowlands have been found. *(ii)* Due to degradation conditions, upland derived DOC showed lower molecular weight DOC than peat-influenced stream DOC and were thus more biolabile. Nonetheless, in general, the molecular weight structure represented that relatively low-molecular DOC was found in all sub-catchments, independent of the morphological parameters and the peatland cover. This might indicate that permafrost degradation and thus a release of low-molecular weight C occurred. Even though, regarding the stable C isotope signature, this trend could not be found. Nevertheless, they point to the assumption that in upland areas an increased degradation occurred. However, more research, which includes the active layer depth over several years, is needed here.

The visual analysis of the lability classes of the DOC showed that (*iii*) upland areas contain more labile DOC, which is preferably utilized by bacteria before utilizing semi-labile DOC. In peaty lowlands, the visual analysis did not show the presence of labile DOC and therefore a reduced degradation rate.

However, the data have to be observed with care, as a single sub-catchment consideration was applied, and thus upstream values were not considered. Furthermore, the storage time may have affected the DOC in the samples and manipulated the results. Moreover, the data only represent one season of the year 2018 and may look different at another time point. Especially, as it was one of the warmest years on record, and thus 2018 did not represent an average year. Although the systematically observed high a250/a365 values may indicate that significant amounts of bioreactive DOC could reach streams from permafrost catchments during a warm summer.

Overall, the results of this work showed that there existed a spatial variability in the DOC dynamic between the sub-catchments and it is of high interest how this continues with further climate change.

References

Abisko Scientific Research Station, 2021; Meterological data from Abisko Observation, daily mean 1985-01-01 – 2020-12-31; Station, Abisko Scientific Research. Obtained by request.

Aitkenhead-Peterson, J. A., W. H. McDowell, and J. C. Neff. 2003. Sources, Production, and Regulation of Allochthonous Dissolved Organic Matter Inputs to Surface Waters. In *Aquatic Ecosystems*, 25–70. USA: Elsevier Science. doi:10.1016/b978-012256371-3/50003-2.

Åkerman, H. J., and M. Johansson. 2008. Thawing permafrost and thicker active layers in sub-arctic Sweden. *Permafrost and Periglacial Processes* 19: 279–292. doi:10.1002/ppp.626.

Al-Kharusi, S. 2021. Broad-Scale Patterns in CDOM and Total Organic Matter Concentrations of Inland Waters - Insights from Remote Sensing and GIS. Doctor, Dept of Physical Geography and Ecosystem Science, University Lund.

Beaupré, S. R. 2015. The Carbon Isotopic Composition of Marine DOC. In *Biogeochemistry of Marine Dissolved Organic Matter: Second Edition*, 335–368. Massachusetts, USA: Academic Press.

Berggren, M., and P. A. Giorgio. 2015. Distinct patterns of microbial metabolism associated to riverine dissolved organic carbon of different source and quality. *Journal of Geophysical Research: Biogeosciences* 120: 989–999. doi:10.1002/2015JG002963.

Berggren, M., H. Laudon, and M. Jansson. 2007. Landscape regulation of bacterial growth efficiency in boreal freshwaters. *Global Biogeochemical Cycles* 21: 1–9. doi:10.1029/2006GB002844.

Berggren, M., J. F. Lapierre, and P. A. Del Giorgio. 2012. Magnitude and regulation of bacterioplankton respiratory quotient across freshwater environmental gradients. *ISME Journal* 6: 984–993. doi:10.1038/ismej.2011.157.

Berggren, M., M. Klaus, B. Panneer Selvam, L. Ström, H. Laudon, M. Jansson, and J. Karlsson. 2018. Quality transformation of dissolved organic carbon during water transit through lakes: Contrasting controls by photochemical and biological processes. *Biogeosciences* 15: 457–470. doi:10.5194/bg-15-457-2018.

Berggren, M., C. Gudasz, F. Guillemette, G. Hensgens, L. Ye, and J. Karlsson. 2020. Systematic microbial production of optically active dissolved organic matter in subarctic lake water. *Limnology and Oceanography* 65: 951–961. doi:10.1002/lno.11362.

Biskaborn, B. K., S. L. Smith, J. Noetzli, H. Matthes, G. Vieira, D. A. Streletskiy, P. Schoeneich, V. E. Romanovsky, et al. 2019. Permafrost is warming at a global scale. *Nature Communications* 10: 1–11. doi:10.1038/s41467-018-08240-4.

Carey, S. K. 2003. Dissolved organic carbon fluxes in a discontinuous permafrost subarctic alpine catchment. *Permafrost and Periglacial Processes* 14: 161–171. doi:10.1002/ppp.444.

Chen, W., and P. J. Wangersky. 1996. Rates of microbial degradation of dissolved organic carbon from phytoplankton cultures. *Journal of Plankton Research* 18: 1521–1533. doi:10.1093/plankt/18.9.1521.

Clymo, R. 1984. The limits to peat bog growth. *Philosophical Transactions of the Royal Society of London. B, Biological Sciences* 303: 605–654. doi:10.1098/rstb.1984.0002.

Cole, J. J., Y. T. Prairie, N. F. Caraco, W. H. McDowell, L. J. Tranvik, R. G. Striegl, C. M. Duarte, P. Kortelainen, et al. 2007. Plumbing the Global Carbon Cycle: Integrating Inland Waters into the Terrestrial Carbon Budget. *Ecosystems* 10: 172–185. doi:10.1007/s10021-006-9013-8.

Coulson, J. C., and J. Butterfield. 1978. An investigation of the biotic factors determining the rates of plant decomposition on blanket bog. *The Journal of Ecology* 66: 631–650.

Drake, T. W., K. P. Wickland, R. G. M. Spencer, D. M. McKnight, and R. G. Striegl. 2015. Ancient low–molecular-weight organic acids in permafrost fuel rapid carbon dioxide production upon thaw. *Proceedings of the National Academy of Sciences* 112: 13946–13951. doi:10.1073/pnas.1511705112.

Drake, T. W., P. A. Raymond, and R. G. M. Spencer. 2018. Terrestrial carbon inputs to inland waters: A current synthesis of estimates and uncertainty. *Limnology and Oceanography Letters* 3: 132–142. doi:10.1002/lol2.10055.

European Arctic | Copernicus. 2021. [ESOTO 2018 | Climate in 2018 | General]. Accessed February 15 from https://climate.copernicus.eu/european-arctic.

Ewing, S. A., J. A. O'Donnell, G. R. Aiken, K. Butler, D. Butman, L. Windham-Myers, and M. Z. Kanevskiy. 2015. Long-term anoxia and release of ancient, labile carbon upon thaw of Pleistocene permafrost. *Geophysical Research Letters* 42: 10730–10738. doi:10.1002/2015GL066296.

Fellman, J. B., D. V. D. Amore, E. Hood, and R. D. Boone. 2008. Fluorescence characteristics and biodegradability of dissolved organic matter in forest and wetland soils from coastal temperate watersheds in southeast Alaska. *Biogeochemistry* 88: 169–184. doi:10.1007/s10533-008-9203-x.

Feuchtmayr, H., T. G. Pottinger, A. Moore, M. M. De Ville, L. Caillouet, H. T. Carter, M. G. Pereira, and S. C. Maberly. 2019. Effects of brownification and warming on algal blooms, metabolism and higher trophic levels in productive shallow lake mesocosms. *Science of the Total Environment* 678: 227–238. doi:10.1016/j.scitotenv.2019.04.105.

Fuchs, G., M. Boll, and J. Heider. 2011. Microbial degradation of aromatic compounds- From one strategy to four. *Nature Reviews Microbiology* 9: 803–816. doi:10.1038/nrmicro2652.

Grieve, I. C. 1991. A model of dissolved organic carbon concentrations in soil and stream waters. *Hydrological Processes* 5: 301–307. doi:10.1002/hyp.3360050310.

Haga, H., Y. Matsumoto, J. Matsutani, M. Fujita, K. Nishida, and Y. Sakamoto. 2005. Flow paths, rainfall properties, and antecedent soil moisture controlling lags to peak discharge in a granitic unchanneled catchment. *Water Resources Research* 41: 1–14. doi:10.1029/2005WR004236.

Harris, S., H. French, J. Heginbottom, G. Johnston, B. Ladanyi, D. Sego, and R. van Everdingen. 1988. *Glossary of permafrost and related ground-ice terms*. Edited by Associate Committee on Geotechnical Research. *Associate Committee on Geotechnical Research, National Research Council of Canada, Ottawa*. National Research Council of Canada.

Van Hees, P. A. W., D. L. Jones, R. Finlay, D. L. Godbold, and U. S. Lundström. 2005. The carbon we do not see - The impact of low molecular weight compounds on carbon dynamics and respiration in forest soils: A review. *Soil Biology and Biochemistry* 37: 1–13. doi:10.1016/j.soilbio.2004.06.010.

Hensgens, G., H. Laudon, M. Peichl, I. A. Gil, Q. Zhou, and M. Berggren. 2020. The role of the understory in litter DOC and nutrient leaching in boreal forests. *Biogeochemistry* 149: 87–103. doi:10.1007/s10533-020-00668-5.

Heslop, J. K., M. Winkel, K. M. Walter Anthony, R. G. M. Spencer, D. C. Podgorski, P. Zito, A. Kholodov, M. Zhang, et al. 2019. Increasing Organic Carbon Biolability With Depth in Yedoma Permafrost: Ramifications for Future Climate Change. *Journal of Geophysical Research: Biogeosciences* 124: 2021–2038. doi:10.1029/2018JG004712.

Hinzman, L. D., N. D. Bettez, W. R. Bolton, F. S. Chapin, M. B. Dyurgerov, C. L. Fastie, B. Griffith, R. D. Hollister, et al. 2005. Evidence and Implications of Recent Climate Change in Northern Alaska and Other Arctic Regions. *Climatic Change* 72: 251–298. doi:10.1007/s10584-005-5352-2.

Hobbie, S. E., J. P. Schimel, S. E. Trumbore, and J. R. Randerson. 2000. Controls over carbon storage and turnover in high-latitude soils. *Global Change Biology* 6: 196–210. doi:10.1046/j.1365-2486.2000.06021.x.

Hodgkins, S. B., M. M. Tfaily, D. C. Podgorski, C. K. McCalley, S. R. Saleska, P. M. Crill, V. I. Rich, J. P. Chanton, et al. 2016. Elemental composition and optical properties reveal changes in dissolved organic matter along a permafrost thaw chronosequence in a subarctic peatland. *Geochimica et Cosmochimica Acta* 187: 123–140. doi:10.1016/j.gca.2016.05.015.

Hope, D., M. F. Billett, and M. S. Cresser. 1994. A review of the export of carbon in river water: Fluxes and processes. *Environmental Pollution* 84: 301–324. doi:10.1016/0269-7491(94)90142-2.

IPCC 2013. Climate Change 2013: The Physical Science Basis. Contribution of Working Group I to the Fifth Assessment Report of the Intergovernmental Panel on Climate Change. *[Stocker, T.F., D. Qin, G.-K. Plattner, M. Tignor, S.K. Allen, J. Boschung, A. Nauels, Y. Xia, V. Bex and P.M. Midgley (eds.)]. Cambridge University Press, Cambridge, United Kingdom and New York, NY, USA, 1535 pp.*

Jiménez, E. M., M. C. P.-M. Peñuela, C. A. Sierra, J. Lloyd, O. L. Phillips, F. H. Moreno, D. Navarrete, A. Prieto, et al. 2014. Journal of Geophysical Research: Biogeosciences. *Journal of Geophysical Research: Biogeosciences* 119: 487–507. doi:10.1002/2013JG002527.

Johansson, M., T. R. Christensen, H. J. Akerman, and T. V. Callaghan. 2006. What determines the current presence or absence of permafrost in the Torneträsk region, a sub-Arctic landscape in Northern Sweden? *AMBIO: A Journal of the Human Environment* 35: 190–197.

John, R. H., A. Stubbins, J. D. Ritchie, E. C. Minor, D. J. Kieber, and K. Mopper. 2008. Absorption spectral slopes and slope ratios as indicators of molecular weight, source, and photobleaching of chromophoric dissolved organic matter. *Limnology and Oceanography* 53: 955–969. doi:10.4319/lo.2009.54.3.1023.

Jonsson, A., J. Karlsson, and M. Jansson. 2003. Sources of carbon dioxide supersaturation in clearwater and humic lakes in northern Sweden. *Ecosystems* 6: 224–235. doi:10.1007/s10021-002-0200-y.

Kanaly, R. A., and S. Harayama. 2000. Biodegradation of high-molecular-weight polycyclic aromatic hydrocarbons by bacteria. *Journal of Bacteriology* 182: 2059–2067. doi:10.1128/JB.182.8.2059-2067.2000.

Kaplan, L. A. 1994. A field and laboratory procedure to collect, process, and preserve fresh-water samples for dissolved organic carbon analysis. *Limnology and Oceanography* 39: 1470–1476. doi:10.4319/lo.1994.39.6.1470.

King, L. 1986. Zonation and Ecology of High Mountain Permafrost in Scandinavia. *Geografiska Annaler: Series A, Physical Geography* 68: 131–139. doi:10.1080/04353676.1986.11880166.

Köhler, S. J., I. Buffam, H. Laudon, and K. H. Bishop. 2008. Climate's control of intra-annual and interannual variability of total organic carbon concentration and flux in two contrasting boreal landscape elements. *Journal of Geophysical Research: Biogeosciences* 113: 1–12. doi:10.1029/2007JG000629.

Lambert, T., A. C. Pierson-Wickmann, G. Gruau, A. Jaffrezic, P. Petitjean, J. N. Thibault, and L. Jeanneau. 2014. DOC sources and DOC transport pathways in a small headwater catchment as revealed by carbon isotope fluctuation during storm events. *Biogeosciences* 11: 3043–3056. doi:10.5194/bg-11-3043-2014.

Lapierre, J. F., F. Guillemette, M. Berggren, and P. A. Del Giorgio. 2013. Increases in terrestrially derived carbon stimulate organic carbon processing and CO 2 emissions in boreal aquatic ecosystems. *Nature Communications* 4: 1–7. doi:10.1038/ncomms3972.

Lundin, E. J., R. Giesler, A. Persson, M. S. Thompson, and J. Karlsson. 2013. Integrating carbon emissions from lakes and streams in a subarctic catchment. *Journal of Geophysical Research: Biogeosciences* 118: 1200–1207. doi:10.1002/jgrg.20092.

Ma, Q., H. Jin, C. Yu, and V. F. Bense. 2019. Dissolved organic carbon in permafrost regions: A review. *Science China Earth Sciences* 62: 349–364. doi:10.1007/s11430-018-9309-6.

Malmer, N., T. Johansson, M. Olsrud, and T. R. Christensen. 2005. Vegetation, climatic changes and net carbon sequestration in a North-Scandinavian subarctic mire over 30 years. *Global Change Biology* 11: 1895–1909. doi:10.1111/j.1365-2486.2005.01042.x.

Mao, R., X.-H. Zhang, S.-Y. Li, and C.-C. Song. 2017. Long-term phosphorus addition enhances the biodegradability of dissolved organic carbon in a nitrogen-limited temperate freshwater wetland. *Science of The Total Environment* 605–606: 332–336. doi:10.1016/j.scitotenv.2017.06.200.

Morris, P. J., and J. M. Waddington. 2011. Groundwater residence time distributions in peatlands: Implications for peat decomposition and accumulation. *Water Resources Research* 47: 1–12. doi:10.1029/2010WR009492.

Mu, C., T. Zhang, Q. Wu, X. Zhang, B. Cao, Q. Wang, X. Peng, and G. Cheng. 2014. Stable carbon isotopes as indicators for permafrost carbon vulnerability in upper reach of Heihe River basin, northwestern China. *Quaternary International* 321: 71–77. doi:10.1016/j.quaint.2013.12.001.

Mzobe, P., M. Berggren, P. Pilesjö, E. Lundin, D. Olefeldt, N. T. Roulet, and A. Persson. 2018. Dissolved organic carbon in streams within a subarctic catchment analysed using a GIS/ remote sensing approach. *PLoS ONE* 13: 1–20. doi:10.1371/journal.pone.0199608.

Mzobe, P., Y. Yan, M. Berggren, P. Pilesjö, D. Olefeldt, E. Lundin, N. T. Roulet, and A. Persson. 2020. Morphometric Control on Dissolved Organic Carbon in Subarctic Streams. *Journal of Geophysical Research: Biogeosciences* 125: 1–16. doi:10.1029/2019JG005348.

O'Leary, M. H. 1988. Carbon Isotopes in Photosynthesis. *BioScience* 38: 328–336. doi:10.2307/1310735.

Olefeldt, D. 2011. Quantity and composition of waterborne carbon transport in subarctic catchments containing peatlands and permafrost. *Doctor*. Department of Geography, McGill University, Montreal.

Olefeldt, D., and N. T. Roulet. 2012. Effects of permafrost and hydrology on the composition and transport of dissolved organic carbon in a subarctic peatland complex. *Journal of Geophysical Research: Biogeosciences* 117: 1–15. doi:10.1029/2011JG001819.

Olefeldt, D., and N. T. Roulet. 2014. Permafrost conditions in peatlands regulate magnitude, timing, and chemical composition of catchment dissolved organic carbon export. *Global Change Biology* 20: 3122–3136. doi:10.1111/gcb.12607.

Olefeldt, D., N. Roulet, R. Giesler, and A. Persson. 2013. Total waterborne carbon export and DOC composition from ten nested subarctic peatland catchments-importance of peatland cover, groundwater influence, and inter-annual variability of precipitation patterns. *Hydrological Processes* 27: 2280–2294. doi:10.1002/hyp.9358.

Peacock, M., C. Freeman, V. Gauci, I. Lebron, and C. D. Evans. 2015. Investigations of freezing and cold storage for the analysis of peatland dissolved organic carbon (DOC) and absorbance properties. *Environmental Sciences: Processes and Impacts* 17: 1290–1301. doi:10.1039/c5em00126a.

Peters, W., A. Bastos, P. Ciais, and A. Vermeulen. 2020. A historical, geographical and ecological perspective on the 2018 European summer drought: Perspective on the 2018 European drought. *Philosophical Transactions of the Royal Society B: Biological Sciences* 375: 1–8. doi:10.1098/rstb.2019.0505.

Peuravuori, J., and K. Pihlaja. 1997. Molecular size distribution and spectroscopic properties of aquatic humic substances. *Analytica Chimica Acta* 337: 133–149. doi:10.1016/S0003-2670(96)00412-6.

Quinton, W. L., and P. Marsh. 1999. A conceptual framework for runoff generation in a permafrost environment. *Hydrological Processes* 13: 2563–2581. doi:org/10.1002/(SICI)1099-1085(199911)13:16.

Ramonet, M., P. Ciais, F. Apadula, J. Bartyzel, A. Bastos, P. Bergamaschi, P. E. Blanc, D. Brunner, et al. 2020. The fingerprint of the summer 2018 drought in Europe on ground-based atmospheric CO 2 measurements: Atmospheric CO 2 anomaly. *Philosophical Transactions of the Royal Society. Series B: Biological Sciences* 375: 1–21. doi:10.1098/rstb.2019.0513.

Reddy, K. J., L. C. Munn, and W. Liyuan. 1997. Chemistry and mineralogy of molybdenum in soils. In *Molybdenum in Agriculture*, 4–22. New York, USA: Cambridge University Press.

Rolfe, M. D., C. J. Rice, S. Lucchini, C. Pin, A. Thompson, A. D. S. Cameron, M. Alston, M. F. Stringer, et al. 2012. Lag phase is a distinct growth phase that prepares bacteria for exponential growth and involves transient metal accumulation. *Journal of Bacteriology* 194: 686–701. doi:10.1128/JB.06112-11.

Romanovsky, V., S. Smith, K. Isaksen, N. Shiklomanov, D. Streletskiy, A. Kholodov, H. Christiansen, D. Drozdov, et al. 2019. Terrestrial permafrost [in "State of the Climate in 2018"]. *Bulletin of the American Meteorological Society* 100(9).

Schaub, M., and C. Alewell. 2009. Stable carbon isotopes as an indicator for soil degradation in an alpine environment (Urseren Valley, Switzerland). *Rapid Communications in Mass Spectrometry* 23: 1499–1507. doi:10.1002/rcm.4030.

Schlesinger, W. H., and E. S. Bernhardt. 2013. *Biogeochemistry: an analysis of global change*. 3. ed. Amsterdam: Elsevier.

Schuur, E. A. G., J. Bockheim, J. G. Canadell, E. Euskirchen, C. B. Field, S. V. Goryachkin, S. Hagemann, P. Kuhry, et al. 2008. Vulnerability of Permafrost Carbon to Climate Change: Implications for the Global Carbon Cycle. *BioScience* 58: 701–714. doi:10.1641/B580807.

Schuur, E. A. G., A. D. McGuire, C. Schädel, G. Grosse, J. W. Harden, D. J. Hayes, G. Hugelius, C. D. Koven, et al. 2015. Climate change and the permafrost carbon feedback. *Nature* 520: 171–179. doi:10.1038/nature14338.

Sebestyen, S. D., M. Funke, and J. B. Cotner. 2021. Sources and biodegradability of dissolved organic matter in two headwater peatland catchments at the Marcell Experimental Forest, northern Minnesota, USA. *Hydrological Processes* 35: 0–37. doi:10.1002/hyp.14049.

Selvam, B. P., J. F. Lapierre, F. Guillemette, C. Voigt, R. E. Lamprecht, C. Biasi, T. R. Christensen, P. J. Martikainen, et al. 2017. Degradation potentials of dissolved organic carbon (DOC) from thawed permafrost peat. *Scientific Reports* 7: 1–9. doi:10.1038/srep45811.

SMHI | Nederbördsmänge (dygn): Alla Stationer - *SMHI | Ladda ner meteorologiska observationer | Nederbördsmänge (dygn): Alla Stationer*. Accessed June 21 from https://www.smhi.se/data/meteorologi/ladda-ner-meteorologiska-observationer/#param=precipitation24HourSum,stations=all,stationid=188800.

Smith, M. W., and D. W. Riseborough. 2002. Climate and the limits of permafrost: A zonal analysis. *Permafrost and Periglacial Processes* 13: 1–15. doi:10.1002/ppp.410.

Spencer, R. G. M., P. J. Mann, T. Dittmar, T. I. Eglinton, C. Mcintyre, R. M. Holmes, N. Zimov, and A. Stubbins. 2015. Detecting the signature of permafrost thaw in Arctic rivers. *Geophysical Research Letters* 42: 2830–2835. doi:10.1002/2015GL063498.Received.

Van Stan, J. T., and A. Stubbins. 2018. Tree-DOM: Dissolved organic matter in throughfall and stemflow. *Limnology and Oceanography Letters* 3: 199–214. doi:10.1002/lol2.10059.

Strand, S. M., H. H. Christiansen, M. Johansson, J. Åkerman, and O. Humlum. 2020. Active layer thickening and controls on interannual variability in the Nordic Arctic compared to the circum-Arctic. *Permafrost and Periglacial Processes* 32: 47–58. doi:10.1002/ppp.2088.

Striegl, R. G., G. R. Aiken, M. M. Dornblaser, P. A. Raymond, and K. P. Wickland. 2005. A decrease in discharge-normalized DOC export by the Yukon River during summer through autumn. *Geophysical Research Letters* 32: 1–4. doi:10.1029/2005GL024413.

Strock, K. E., N. Theodore, W. G. Gawley, A. C. Ellsworth, and J. E. Saros. 2017. Increasing dissolved organic carbon concentrations in northern boreal lakes: Implications for lake water transparency and thermal structure. *Journal of Geophysical Research: Biogeosciences* 122: 1022–1035. doi:10.1002/2017JG003767.

Su, Y., F. Chen, and Z. Liu. 2015. Comparison of optical properties of chromophoric dissolved organic matter (CDOM) in alpine lakes above or below the tree line: Insights into sources of CDOM. *Photochemical and Photobiological Sciences* 14: 1047–1062. doi:10.1039/c4pp00478g.

Tang, J., P. A. Miller, A. Persson, D. Olefeldt, P. Pilesjö, M. Heliasz, M. Jackowicz-Korczynski, Z. Yang, et al. 2015. Carbon budget estimation of a subarctic catchment using a dynamic ecosystem model at high spatial resolution. *Biogeosciences* 12: 2791–2808. doi:10.5194/bg-12-2791-2015.

Tarnocai, C., J. G. Canadell, E. A. G. Schuur, P. Kuhry, G. Mazhitova, and S. Zimov. 2009. Soil organic carbon pools in the northern circumpolar permafrost region. *Global Biogeochemical Cycles* 23: 1–11. doi:10.1029/2008GB003327.

Tavakkoli, E., P. Rengasamy, E. Smith, and G. K. Mcdonald. 2015. The effect of cation-anion interactions on soil pH and solubility of organic carbon. *European Journal of Soil Science* 66: 1054–1062. doi:10.1111/ejss.12294.

Tranvik, L. J., J. A. Downing, J. B. Cotner, S. A. Loiselle, R. G. Striegl, T. J. Ballatore, P. Dillon, K. Finlay, et al. 2009. Lakes and reservoirs as regulators of carbon cycling and climate. *Limnology and Oceanography* 54: 2298–2314. doi:10.4319/lo.2009.54.6_part_2.2298.

Vitale, C. M., and A. Di Guardo. 2019. A review of the predictive models estimating association of neutral and ionizable organic chemicals with dissolved organic carbon. *Science of the Total Environment* 666: 1022–1032. doi:10.1016/j.scitotenv.2019.02.340.

Walker, B. D., S. Griffin, and E. R. M. Druffel. 2017. Effect of Acidified Versus Frozen Storage on Marine Dissolved Organic Carbon Concentration and Isotopic Composition. *Radiocarbon* 59: 843–857. doi:10.1017/RDC.2016.48.

Wauthy, M., and M. Rautio. 2020. Permafrost thaw stimulates primary producers but has a moderate effect on primary consumers in subarctic ponds. *Ecosphere* 11: 1–16. doi:10.1002/ecs2.3099.

Wilson, J., J. Munizzi, and A. M. Erhardt. 2020. Preservation methods for the isotopic composition of dissolved carbon species in non-ideal conditions. *Rapid Communications in Mass Spectrometry* 34: 1–11. doi:10.1002/rcm.8903.

Wynn, J. G., M. I. Bird, and V. N. L. Wong. 2005. Rayleigh distillation and the depth profile of 13C/ 12C ratios of soil organic carbon from soils of disparate texture in Iron Range National Park, Far North Queensland, Australia. *Geochimica et Cosmochimica Acta* 69: 1961–1973. doi:10.1016/j.gca.2004.09.003.

Xenopoulos, M. A., R. T. Barnes, K. S. Boodoo, D. Butman, N. Catalán, S. C. D'Amario, C. Fasching, D. N. Kothawala, et al. 2021. How humans alter dissolved organic matter composition in freshwater: relevance for the Earth's biogeochemistry. *Biogeochemistry*: 1–26. doi:10.1007/s10533-021-00753-3.

Yang, K., and B. Xing. 2009. Adsorption of fulvic acid by carbon nanotubes from water. *Environmental Pollution* 157: 1095–1100. doi:10.1016/j.envpol.2008.11.007.

Zhang, T., R. Barry, K. Knowles, F. Ling, and R. Armstrong. 2003. Distribution of seasonally and perennially frozen ground in the Northern Hemisphere. *Proceedings of the 8th International Conference on Permafrost* 2: 1289–1294.

Zhao, L., C. Xie, D. Yang, and T. Zhang. 2021. Ground Temperature and Active Layer Regimes and Changes. In *Arctic Hydrology, Permafrost and Ecosystems*, 441–470. Cham: Switzerland: Springer Cham. doi:10.1007/978-3-030-50930-9_15.

Appendix

Appendix I

Daily mean precipitation pattern (mm) for the month July and August from 2015-2020 (excluding 2018) and individual pattern for 2018.

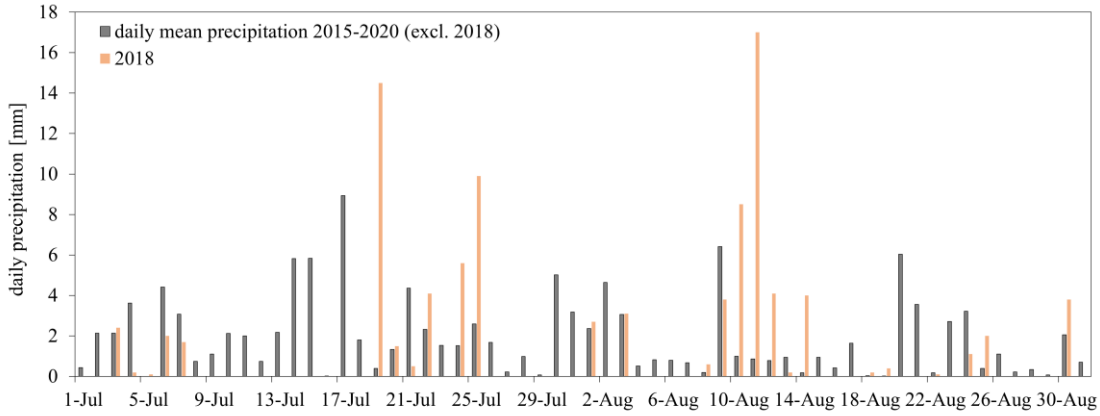

Figure AI. *Bars showing mean daily precipitation (mm) for the month July and August from 2015-2020 (excluding 2018) and individual for 2018. Data were provided by SMHI (SMHI | Nederbördsmänge (dygn): Alla Stationer - assessed June 2021).*

Appendix II

Correlation between morphological variables and peatland cover of the sub-catchments.

Table AII. *Morphological variable and there correlation. A significance level of 0.01 was used. Significant codes p-value ≤ 0.0001 "***", p-value ≤ 0.001 "**", p-value ≤ 0.01 "*". Morphological data from Mzobe et al. (2020). Peatland cover from are from (Olefeldt et al. 2013). For all variables n = 58. Numbers represent the tau correlation coefficient.*

	Elevation	**Relief**	**Slope**	**Area**	**Peatland cover**
Elevation		0.71 ***	0.71 ***	0.28 *	-0.44 ***
relief			0.64 ***	0.57 ***	-0.49 ***
Slope				0.22	-0.60 ***
Area					-0.15